ESAIM: M2AN 57 (2023) 1029–1062
https://doi.org/10.1051/m2an/2023014

**ESAIM: Mathematical Modelling and Numerical Analysis**
www.esaim-m2an.org

# STABLE RECONSTRUCTION OF DISCONTINUOUS SOLUTIONS TO THE CAUCHY PROBLEM IN STEADY-STATE ANISOTROPIC HEAT CONDUCTION WITH NON-SMOOTH COEFFICIENTS

Mihai Bucataru[1,2], Iulian Cimpean[1,3] and Liviu Marin[1,2,*]

**Abstract.** We study the recovery of the missing discontinuous/non-smooth thermal boundary conditions on an inaccessible portion of the boundary of the domain occupied by a solid from Cauchy data prescribed on the remaining boundary assumed to be accessible, in case of stationary anisotropic heat conduction with non-smooth/discontinuous conductivity coefficients. This inverse boundary value problem is ill-posed and, therefore, should be regularized. Consequently, a stabilising method is developed based on *a priori* knowledge on the solution to this inverse problem and the smoothing feature of the direct problems involved. The original problem is transformed into a control one which reduces to solving an appropriate minimisation problem in a suitable function space. The latter problem is tackled by employing an appropriate variational method which yields a gradient-type iterative algorithm that consists of two direct problems and their corresponding adjoint ones. This approach yields an algorithm designed to approximate specifically merely $L^2$–boundary data in the context of a non-smooth/discontinuous anisotropic conductivity tensor, hence both the notion of solution to the direct problems involved and the convergence analysis of the approximate solutions generated by the algorithm proposed require special attention. The numerical implementation is realised for two-dimensional homogeneous anisotropic solids using the finite element method, whilst regularization is achieved by terminating the iteration according to two stopping criteria.

**Mathematics Subject Classification.** 80A23, 65N20, 65N21, 65N30, 35Q93, 35R30.

Received September 1, 2022. Accepted February 12, 2023.

## 1. Introduction

Two major issues usually occur in real life problems related to stationary heat conduction, namely the dependence of the thermal conductivity tensor associated with the solid body considered on a preferred direction, *i.e.* the thermal anisotropy of the solid, and the inaccessibility of some portions of the boundary of the solid

*Keywords and phrases.* Inverse Cauchy problem, Anisotropic heat conduction, Control problem, Minimisation problem, Regularization, Finite element method.

[1] Department of Mathematics, Faculty of Mathematics and Computer Science, University of Bucharest, 14 Academiei, 010014 Bucharest, Romania

[2] "Gheorghe Mihoc – Caius Iacob" Institute of Mathematical Statistics and Applied Mathematics of the Romanian Academy, 13 Calea 13 Septembrie, 050711 Bucharest, Romania

[3] Institute of Mathematics of the Romanian Academy, 21 Calea Griviţei, 010702 Bucharest, Romania

*Corresponding author: liviu.marin@fmi.unibuc.ro; marin.liviu@gmail.com

that actually implies incomplete boundary measurements and hence a lack of boundary conditions. The former issue stems from a realistic modelling of steady-state heat transfer in solids and results in the so-called Laplace–Beltrami or anisotropic Laplace equation, whilst the latter one is usually overcome by over-prescribed (Cauchy) data on the accessible part of the boundary, *i.e.* both the temperature and the normal heat flux are measured, which yields a classical inverse boundary value problem, also referred to as the Cauchy problem in steady-state heat conduction. It is well-known that such inverse Cauchy problems are ill-posed, in the sense that the existence, uniqueness and stability of their solutions are not always guaranteed, see *e.g.* Hadamard [23]. Therefore, an important requirement would be to propose suitable methods for obtaining a unique, accurate, convergent and stable solution to the inverse and ill-posed Cauchy problem in steady-state anisotropic heat conduction.

Despite that most of the studies available in the literature have been devoted to the inverse Cauchy problem for Laplace's equation (stationary isotropic heat conduction), the corresponding inverse boundary value problem for the Laplace–Beltrami equation (steady-state anisotropic heat conduction) has been addressed by numerous researchers both theoretically and numerically in the last two decades. The iterative algorithm of Kozlov *et al.* [30], originally proposed for the Laplace equation, was adapted to solving Cauchy problems with and without domain singularities in two-dimensional anisotropic heat conduction, using the boundary element method (BEM), by Mera *et al.* [37,38]. The reconstruction of solutions to second-order elliptic equations, for which the Laplace–Beltrami equation is a particular case, from Cauchy data available on a portion of the boundary, was achieved *via* an alternating iterative algorithm proposed by Johansson [29], who also proved the convergence of the numerical solution to the exact one in a weighted $L^2$-space. The nonlinear Cauchy problem for the anisotropic Laplace equation, for which the thermal conductivity tensor is assumed to depend on the temperature field, was transformed into a similar inverse problem, however for the Laplace equation, together with a sequence of nonlinear scalar equation and was solved *via* an iterative procedure with and without relaxation and the BEM by Essaouini *et al.* [15,16]. Andrieux *et al.* [3,4] approached the Cauchy problem in anisotropic heat conduction by minimising an energy-like functional and implemented this method in two dimensions. Since this method produces unstable results for perturbed data, Rischette *et al.* [41, 42] performed a numerical analysis of the energy-like method accounting for noisy Cauchy data and proposed suitable regularization procedures based upon *a priori* and *a posteriori* error estimates. Chakib and Nachaoui [13] reformulated the Cauchy problem for the anisotropic Laplace equation as an optimal control problem, provided that some regularity assumptions on the data are fulfilled, proved the existence of an optimal solution to this problem and retrieved its numerical approximation using the finite element method (FEM). Jin *et al.* [28] and Marin [32] solved a similar inverse Cauchy problem by employing the method of fundamental solutions (MFS) together with the truncated singular value decomposition (SVD) and the iterative algorithms of Kozlov *et al.* [30], respectively, whereas some relaxation procedures of the above mentioned MFS-based algorithms were also proposed by Marin [33]. Aboulaïch *et al.* [1] reformulated the inverse Cauchy problem for Laplace–Beltrami's equation as an optimal control one which is based on a cost functional with a fading regularization term inspired by domain decomposition methods. The Cauchy problem for a general elliptic equation, which generalises the anisotropic heat conduction equation, was approached by [26] *via* a gradient method and both the finite-difference method (FDM) and the BEM. Azaïez *et al.* [5] investigated the Cauchy problem for the anisotropic Laplace equation using the Steklov–Poincaré approach, discretised the resulting variational problem by the FEM and regularized/stabilised the problem by the Lavrentiev method. In the Steklov–Poincaré variational setting, Ben Belgacem *et al.* [7] applied the Lavrentiev method for regularizing the Cauchy problem for the Laplace–Beltrami equation and provided local convergence rates for both bias and variance errors without any particular smoothness assumption on the exact solution. A rigorous numerical analysis of the corresponding FEM approximation of the solution to this inverse problem, in the same framework, was later realised by Ben Belgacem *et al.* [8], who also proved the convergence of the global bias-variance error. Habbal and Khallel [21, 22] reformulated the inverse Cauchy problem for Laplace–Beltrami's equation as a control one and this resulted in a Nash game of static nature with complete information involving both the Dirichlet and the Neumann gap costs. The same Cauchy problem in two and three dimensions was solved, in a stable manner, by using the Tikhonov regularization method and

the truncated SVD, in conjunction with the singular boundary method, by Gu *et al.* [19, 20]. Dardé [14] investigated the iterated quasi-reversibility method to regularize ill-posed elliptic and parabolic problems, including the Laplace–Beltrami equation, demonstrated the convergence of the regularized solution to the exact one and also proposed a strategy to deal efficiently with noisy data. Baravdish *et al.* [6] proposed an iterative procedure for the stable reconstruction of the solution to a second-order elliptic equation – for which Laplace–Beltrami's equation is yet again a particular case – in a doubly-connected domain from Cauchy data available on the outer boundary and also showed the convergence and stability of this method. A dual regularization method that is closely related to the Kohn–Vogelius minimisation and uses a functional which acts on the space of data, was proposed by Caubet and Dardé [12]. Marin [34] reformulated the inverse Cauchy problem for the anisotropic Laplace equation in the form of a control problem for very weak solutions and applied a variational approach which relies upon the Landweber–Fridman iteration. The fading regularization method was successfully combined with the BEM and the MFS by Voinea-Marinescu and Marin [46] and [47], respectively, to solve stably the Cauchy problem for Laplace–Beltrami's equation in two- and three-dimensions. Ben Belgacem *et al.* [9] investigated the fully discrete FEM approximation of the Cauchy problem associated with the anisotropic Laplace equation corresponding to the variational formulation which stems from the Kohn–Vogelius duplication framed into the Steklov–Poincaré condensation approach, derived a bound of the error with respect to the mesh-size and the Lavrentiev regularization parameter and obtained sharp local FEM estimates. Recently, Bucataru *et al.* [11] approached the inverse Cauchy problem in steady-state anisotropic heat conduction with data in appropriate fractional Sobolev spaces by reformulating it as a control problem with respect to the temperature on the inaccessible boundary. The later problem reduced to the minimisation of a corresponding cost functional defined on a fractional Sobolev space and is solved by a gradient method and the FDM.

At this point, we strongly emphasize that, in all of the aforementioned works, the thermal conductivity tensor is assumed to be smooth, *i.e.* at least from $\mathrm{W}^{1,\infty}$. Also, apart from the works of Marin [34], where the solution is sought in $\mathrm{L}^2$ and the unknown Dirichlet data is assumed to belong to $\mathrm{H}^{1/2}$, and Mera *et al.* [38], where the prescribed boundary data is allowed to exhibit discontinuities at known locations, in all of the papers mentioned above, the space of solutions considered for the Cauchy problem for Laplace–Beltrami's equation is $\mathrm{H}^1$. Hence the main aim of this paper is to show that the inverse Cauchy problem in anisotropic heat conduction can be solved stably under much lower regularity assumptions as explained in Section 2. These assumptions made upon the thermal conductivity tensor are motivated by the existence of some layered materials exhibiting thermal properties, such as the so-called coated materials, see *e.g.* Ma *et al.* [31], Trevisan *et al.* [45] and the references therein. In this case, by applying a certain anisotropic thermal conductive thin coating over a material, referred to as the substrate, the effective thermal conductivity of the layered material is either enhanced or decreased accordingly when compared to that of the substrate only.

In this paper, we investigate the Cauchy problem associated with the Laplace–Beltrami equation for a wide class of anisotropic solids that account for defects or discontinuities of the thermal conductivity tensor apart from an arbitrarily small vicinity of the boundary. More precisely, in the framework of stationary anisotropic heat conduction with a symmetric and positive definite thermal conductivity tensor satisfying some relaxed regularity conditions, see Assumptions (A1)–(A4), one of our main aims is to design a specific convergent and stable iterative method for approximating the unknown discontinuous/irregular thermal boundary conditions (*e.g.*, step functions like or $\mathrm{L}^2$-integrable boundary temperatures) on an inaccessible boundary of the domain occupied by a solid from the knowledge of compatible Cauchy data available on the remaining and accessible boundary. It should be mentioned that the current approach is different from the recent work of Bucataru *et al.* [11], where the coefficients are assumed to be smooth, the solutions are sought in the Sobolev space $\mathrm{H}^1$ and the numerical approach is based on the FDM under even more severe regularity assumptions, whereas in the present study the regularity conditions on the conductivity tensor are more relaxed, hence allowing for the presence of discontinuities/irregularities in the conductivity coefficients, whilst the solutions are sought in the space of square-integrable functions $\mathrm{L}^2$.

The novelty and originality of the present study are summarised as follows:

(i) The notion of weak solutions to two specific direct problems of interest (2.4) and (2.5) is reconsidered under the aforementioned assumptions and, instead, the so-called very weak solutions to these direct problems with $L^2$–Dirichlet (boundary temperature) control data are introduced in a rigorous manner in the spirit of, for example, Berggren [10] or Marin [34], see Definitions 2.3 and 2.4.
(ii) The notion of well-posedness for the above direct problems (2.4) and (2.5) is defined rigorously in this context, see Proposition 2.5.
(iii) The so-called compatibility of the over-specified Cauchy data, see Assumption (A4), is rigorously justified by Proposition 2.6.
(iv) In this function space setting, the original inverse problem is transformed into a control one which reduces to minimising an appropriate cost functional with respect to the $L^2$–boundary temperature control, see (3.1). Note that the minimisation functional considered in the present approach, see (3.2), measures the $L^2$–gap between the exact and reconstructed temperatures in the domain and not on the boundary as usually considered, see Marin [34] and the references therein.
(v) The minimisation problem is tackled *via* an appropriate variational method in a less regular framework which allows for proving the strict convexity of the cost functional (3.2) and hence yields a formula for its Fréchet derivative, see Theorem 3.1.
(vi) This approach together with the crucial Proposition 2.1 provides one with a gradient-type iterative method (3.24)–(3.27) that consists of two direct problems and their two corresponding adjoint ones and represents a weaker, *i.e.* relaxed, version of the gradient descent method recently developed by Bucataru *et al.* [11].
(vii) Although the corresponding functional is strictly convex, it is not strongly convex and, therefore, the convergence of the proposed algorithm requires special attention, as well a non-standard approach, see Theorem 4.1. Despite that the algorithm herein is parameter-dependent, an explicit admissible range for the corresponding relaxation parameter is also provided, whilst its calculation, at each iteration, is not expensive.

The paper is organized as follows: In Section 2.1 the Cauchy problem under consideration is briefly presented, whilst the regularity assumptions made on the anisotropic conductivity tensor and the Cauchy data are also discussed in detail and justified rigorously. The notions of very weak solutions to and well-posedness of two direct problems of interest, referred to as control problems, with $L^2$-boundary temperature on a part of the boundary are introduced in a rigorous manner in Section 2.2. The original inverse boundary value problem is reformulated as a control problem and the latter is reduced to the minimisation of a corresponding cost functional in Section 3.1. It is proved, in Section 3.2, that this functional is strictly convex and twice Fréchet differentiable, and this yields the gradient algorithm described in Section 3.3. In Section 4 the convergence of the resulting algorithm is demonstrated and the admissible range for the corresponding relaxation parameter is discussed. The FEM approximation for two-dimensional problems for Laplace–Beltrami's equation, the convergence of the FEM solution of the minimisation problem and that of the FEM approximate gradient to their exact counterparts are presented in Section 5. The accuracy, convergence, stability and robustness of the proposed iterative procedure are thoroughly analysed in Section 6, for three examples for the two-dimensional Cauchy problem for a solid with a possible non-smooth thermal anisotropy. Section 7 provides some concluding remarks as well as possible future work.

## 2. Problem formulation

### 2.1. Assumptions

Consider a solid occupying the bounded domain $\Omega \subset \mathbb{R}^d$, $d \in \{2,3\}$, with a $C^2$ boundary $\partial\Omega = \Gamma_0 \cup \Gamma_1$ such that $\overline{\Gamma}_0 \cap \overline{\Gamma}_1 = \varnothing$, $\varnothing \neq \Gamma_j \subsetneq \partial\Omega$, $j = 0, 1$, and $\text{meas}(\Gamma_0) > 0$. It is expected that the $C^2$ regularity of the domain $\Omega$ could, in principle, be replaced by another type of regularity, *e.g.*, Lipschitz regularity together with an exterior ball condition, however this is not pursued here. We also assume that this solid body is characterised

by a symmetric and positive definite anisotropic thermal conductivity tensor $\mathbf{K} = \big(k_{ij}\big)_{i,j=\overline{1,d}} : \overline{\Omega} \longrightarrow \mathbb{R}^{d\times d}$. Concerning the regularity of $\mathbf{K}$, the aim is to impose as few restrictions as possible and boundedness would be ideal. Since (weak) derivatives of various solutions at the boundary need to be calculated rigorously, certain regularity conditions on $\mathbf{K}$ have to be imposed at least in a neighbourhood of the boundary. Hence the following regularity assumptions are made on the thermal conductivity tensor:

(A1) $k_{ij} \in \mathrm{L}^\infty(\Omega)$, $i,j = \overline{1,d}$.
(A2) There exists $\varepsilon > 0$ such that $k_{ij}$, $i,j = \overline{1,d}$, are Lipschitz functions in $\overline{\Omega}_\varepsilon := \big\{\mathbf{x} \in \overline{\Omega} \;\big|\; \mathrm{dist}(\mathbf{x}, \partial\Omega) \leq \varepsilon\big\}$.

In particular, a wide class of models that account for defects or discontinuities of the thermal conductivity tensor apart from an arbitrarily small vicinity of the boundary, is covered.

In the absence of heat sources, the temperature field $u$ in the solid of interest satisfies the homogeneous steady-state anisotropic heat conduction in $\Omega$, see Özişik [40], namely

$$\mathscr{L}u := -\nabla \cdot \big(\mathbf{K}\nabla u\big) = 0 \quad \text{in } \Omega\,. \tag{2.1}$$

It is important to mention that, due the relaxed regularity of $\mathbf{K}$, the operator $\mathscr{L}$ acting on smooth functions makes sense only in divergence form and hence it should be regarded as a first-order object on such a class of test functions. Clearly, $\mathscr{L}$ is also well-defined in divergence form on elements $u \in \mathrm{H}^1(\Omega)$. However, the current problem investigated is even more degenerate: Solutions to equation (2.1) will be sought merely in $\mathrm{L}^2(\Omega)$ and hence $\mathscr{L}$ should be regarded in an even much weaker sense, *e.g.*, as a zeroth-order operator by means of its dual $\mathscr{L}^*$ acting on smooth functions. However, the latter operator does not make sense either unless it is regarded in divergence form. Consequently, a first major aim of this paper is to justify rigorously that equation (2.1) really makes sense in the space of square-integrable functions $\mathrm{L}^2(\Omega)$ under the weak regularity Assumptions (A1) and (A2) made on $\mathbf{K}$. Clearly, this low regularity context also raises several issues and restrictions on the numerical method to be employed and its convergence analysis. For example, the FDM is trivially excluded. Briefly, these are the main challenges and difficulties to be tackled in this paper. In addition, the present approach should be compared to the recent work of Bucataru *et al.* [11], where the coefficients are assumed to be smooth, the solutions are sought in the Sobolev space $\mathrm{H}^1(\Omega)$ and the numerical approach is based on the FDM under even more severe regularity assumptions.

We further let $\boldsymbol{\nu}$ be the unit outward normal vector to $\partial\Omega$ and define the normal heat flux (Neumann condition) on $\partial\Omega$ by

$$q \equiv \mathscr{N}_{\boldsymbol{\nu}} u := \boldsymbol{\nu} \cdot \big(\mathbf{K}\nabla u\big) \quad \text{on } \partial\Omega\,. \tag{2.2}$$

The knowledge of suitable boundary conditions on the entire boundary $\partial\Omega$ yields the corresponding direct problems for the thermal equilibrium equation (2.1) and, at the same time, enables one to determine the temperature distribution in the domain, as well as the complementary unknown boundary conditions. It is well-known that such direct problems have a unique weak solution which depends continuously on the data [44], *i.e.* they are well-posed in the sense of Hadamard [23].

Herein, we consider the more realistic and interesting case when both the temperature and the normal heat flux are prescribed only on a part of the boundary assumed to be accessible, say $\Gamma_0 \subsetneq \partial\Omega$, whilst the boundary $\Gamma_1 := \partial\Omega \setminus \Gamma_0$ is assumed to be inaccessible for measurements and hence no boundary conditions are available on $\Gamma_1$. More precisely, we investigate the so-called Cauchy problem in steady-state anisotropic heat conduction given by the partial differential equation (2.1) and the following boundary conditions on $\Gamma_0$, also known as Cauchy data on $\Gamma_0$,

$$u = u^* \quad \text{on } \Gamma_0 \qquad \text{and} \qquad \mathscr{N}_{\boldsymbol{\nu}} u = q^* \quad \text{on } \Gamma_0\,, \tag{2.3}$$

where the prescribed temperature and normal heat flux on $\Gamma_0$ are assumed to satisfy the regularity conditions:

(A3) $u^* \in \mathrm{H}^{1/2}(\Gamma_0)$ and $q^* \in \mathrm{H}^{-1/2}(\Gamma_0)$.

Recall that in real-life applications, $u^*$ and $q^*$ are measured quantities and such measurements are usually taken at specific locations on the boundary $\Gamma_0$. In particular, it would be preferable that the real-life model corresponds

to a Neumann data $q^*$ which is a function on $\Gamma_0$, *e.g.*, $q^* \in \mathrm{L}^2(\Gamma_0)$. Clearly, Assumption (A3) is more relaxed, namely it is assumed that $q^*$ can be measured only by testing it (by duality) with functions from $\mathrm{H}^{1/2}(\Gamma_0)$. The option for such a function space for $q^*$ leads immediately to the natural choice $u^* \in \mathrm{H}^{1/2}(\Gamma_0)$. Analogously, a more relaxed function space for $u^*$, *e.g.*, $\mathrm{L}^2(\Gamma_0)$, could lead to an extremely singular or even undefined Neumann data $q^*$ on $\Gamma_0$, for which real measurements would be unfeasible. Therefore, Assumption (A3) is a natural choice that is also general enough to allow for certain singularities on $\Gamma_0$. However, even if (A3) holds true, it turns out that the unknown solution in $\Omega$ may exhibit a much more singular behaviour especially in the vicinity of the inaccessible boundary $\Gamma_1$, where the Neumann derivative is allowed to blow up, see Proposition 2.6. Consequently, the following assumption is made:

(A4) The prescribed Cauchy data $\left(u^*, q^*\right) \in \mathrm{H}^{1/2}(\Gamma_0) \times \mathrm{H}^{-1/2}(\Gamma_0)$ are *compatible* with an unknown Dirichlet data $v^* \in \mathrm{L}^2(\Gamma_1)$, in the sense that there exists a *very weak solution* to (2.1), $u \in \mathrm{L}^2(\Omega)$, corresponding to the triplet $\left(u^*, q^*, v^*\right)$ in a distributional sense which resembles to, *e.g.*, Berggren [10] or Marin [34]. However, since the possible presence of non-smooth coefficients has been accounted for, some additional issues need to be considered and these are addressed in detail in Section 2.2.

We note that, for a sufficiently smooth thermal conductivity tensor $\mathbf{K}$, as well as compatible Cauchy data on $\Gamma_0$, the uniqueness of the solution to the Cauchy problem (2.1) and (2.3) is guaranteed by Holmgren's uniqueness theorem [27]. Nonetheless, the algorithm proposed in this study is constructed such that it always provides us with a unique specific and regularized solution, hence allowing for discarding the assumption of a unique solution to inverse problem (2.1) and (2.3). However, we recall that herein the thermal conductivity tensor could also be non-smooth and hence Holmgren's result does not apply directly.

## 2.2. Very weak solutions and well-posedness

Next, we introduce the notion of very weak solutions to a couple of direct problems of interest, prove in this context that these problems are well-posed, and discuss the compatibility of this type of solutions with the main numerical algorithm presented in Section 3.3, as well as the assumptions made (A1)–(A4). To do so, for a given boundary temperature control $v \in \mathrm{L}^2(\Gamma_1)$, consider the following direct problems, also referred to as control problems,

$$\mathscr{L} u^{(1)}(v) = 0 \ \text{ in } \Omega\,, \quad u^{(1)}(v) = u^* \ \text{ on } \Gamma_0\,, \quad u^{(1)}(v) = v \ \text{ on } \Gamma_1 \tag{2.4}$$

and

$$\mathscr{L} u^{(2)}(v) = 0 \ \text{ in } \Omega\,, \quad \mathscr{N}_{\boldsymbol{\nu}} u^{(2)}(v) = q^* \ \text{ on } \Gamma_0\,, \quad u^{(2)}(v) = v \ \text{ on } \Gamma_1\,. \tag{2.5}$$

To make the forthcoming computations easy to follow, we further adopt the following convention

$$\int_{\Gamma_i} v\, w \,\mathrm{d}\sigma \coloneqq {}_{\mathrm{H}^{-1/2}(\Gamma_i)}\langle v,\, w\rangle_{\mathrm{H}^{1/2}(\Gamma_i)}\,, \quad \forall\, v \in \mathrm{H}^{-1/2}(\Gamma_i)\,, \quad \forall\, w \in \mathrm{H}^{1/2}(\Gamma_i)\,, \quad i = 0, 1, \tag{2.6}$$

and recall that relation (2.6) becomes rigorous for any $v \in \mathrm{L}^2(\Gamma_i)$, $i = 0, 1$.

**Step I: Heuristic approach.** Formally, on multiplying the partial differential equation in (2.4) by a function $\psi \in \mathrm{H}^2(\Omega)$, integrating over $\Omega$ and using integration by parts, the following yet non-rigorous Green's formula is obtained

$$\begin{aligned} 0 &= \int_\Omega \left(\mathscr{L} u^{(1)}(v)\right) \psi \,\mathrm{d}\mathbf{x} \\ &= \int_\Omega u^{(1)}(v)\, \left(\mathscr{L}^* \psi\right) \,\mathrm{d}\mathbf{x} - \int_{\partial\Omega} \left(\mathscr{N}_{\boldsymbol{\nu}} u^{(1)}(v)\right) \psi \,\mathrm{d}\sigma + \int_{\partial\Omega} u^{(1)}(v)\, \left(\mathscr{N}_{\boldsymbol{\nu}}^* \psi\right) \,\mathrm{d}\sigma\,, \quad \forall\, \psi \in \mathrm{H}^2(\Omega)\,, \end{aligned} \tag{2.7}$$

where $\mathscr{L}^*$ and $\mathscr{N}_{\boldsymbol{\nu}}^*$ are the adjoint operators to $\mathscr{L}$ and $\mathscr{N}_{\boldsymbol{\nu}}$, respectively. Note that, in the current case, $\mathscr{L}^* u \coloneqq -\nabla \cdot \left(\mathbf{K}^{\mathsf{T}} \nabla u\right) \equiv -\nabla \cdot \left(\mathbf{K} \nabla u\right) =: \mathscr{L} u$ and $\mathscr{N}_{\boldsymbol{\nu}}^* u \coloneqq \boldsymbol{\nu} \cdot \left(\mathbf{K}^{\mathsf{T}} \nabla u\right) \equiv \boldsymbol{\nu} \cdot \left(\mathbf{K} \nabla u\right) =: \mathscr{N}_{\boldsymbol{\nu}} u$. The right-hand side of (2.7) could be made rigorous as soon as $u^{(1)}(v) \in \mathrm{L}^2(\Omega)$ and $\psi\big|_{\partial\Omega} = 0$, provided that the conductivity

tensor $\mathbf{K}$ is smooth in $\overline{\Omega}$, *e.g.*, $k_{ij}$, $i,j=\overline{1,d}$, are Lipschitz functions in $\overline{\Omega}$. However, this is not the case according to Assumptions (A1) and (A2) as $k_{ij}$, $i,j=\overline{1,d}$, are Lipschitz functions only in a neighbourhood of $\partial\Omega$ and just bounded functions otherwise. Clearly, this is an inconvenience that should be overcome. The key idea though is to continue with the heuristic approach and regard $\mathscr{L}^*\psi$ in (2.7) as a test function $w\in \mathrm{L}^2(\Omega)$, namely take $\psi_w\in \mathrm{H}^1_0(\Omega)$ to be the weak solution to the following well-posed problem in $\mathrm{H}^1_0(\Omega)$

$$\mathscr{L}^*\psi_w = w \ \text{ in } \Omega\,, \quad \psi_w = 0 \ \text{ on } \partial\Omega\,. \tag{2.8}$$

By using the weak solution to problem (2.8), $\psi_w$, instead of $\psi$ in (2.7), the latter relation is reformulated as

$$\begin{aligned}\int_\Omega u^{(1)}(v)\,w\,\mathrm{d}\mathbf{x} &= -\int_{\Gamma_0} u^{(1)}(v)\,(\mathscr{N}^*_{\boldsymbol{\nu}}\psi_w)\,\mathrm{d}\sigma - \int_{\Gamma_1} u^{(1)}(v)\,(\mathscr{N}^*_{\boldsymbol{\nu}}\psi_w)\,\mathrm{d}\sigma,\\ &= -\int_{\Gamma_0} u^*\,(\mathscr{N}^*_{\boldsymbol{\nu}}\psi_w)\,\mathrm{d}\sigma - \int_{\Gamma_1} v\,(\mathscr{N}^*_{\boldsymbol{\nu}}\psi_w)\,\mathrm{d}\sigma\,, \quad \forall\ w\in \mathrm{L}^2(\Omega)\end{aligned} \tag{2.9}$$

and the last equality becomes well-defined as long as $\mathscr{N}^*_{\boldsymbol{\nu}}\psi_w\in \mathrm{L}^2(\partial\Omega)$.

In case of the second control problem (2.5), for $w\in \mathrm{L}^2(\Omega)$, we consider the following problem

$$\mathscr{L}^*\varphi_w = w \ \text{ in } \Omega\,, \quad \mathscr{N}^*_{\boldsymbol{\nu}}\varphi_w = 0 \ \text{ on } \Gamma_0\,, \quad \varphi_w = 0 \ \text{ on } \Gamma_1 \tag{2.10}$$

which is well-posed in the Hilbert space $\mathrm{H}^1_{00}(\Omega) := \big\{v\in \mathrm{H}^1(\Omega)\ \big|\ \mathscr{N}^*_{\boldsymbol{\nu}}v\big|_{\Gamma_0} = 0\,,\, v\big|_{\Gamma_1} = 0\big\}$ endowed with the scalar product from $\mathrm{H}^1(\Omega)$. Proceeding similarly to the control problem (2.4), the following reformulation of Green's formula for the control problem (2.5) is retrieved

$$\begin{aligned}\int_\Omega u^{(2)}(v)\,w\,\mathrm{d}\mathbf{x} &= \int_{\partial\Omega}\Big(\mathscr{N}^*_{\boldsymbol{\nu}}u^{(2)}(v)\Big)\,\varphi_w\,\mathrm{d}\sigma - \int_{\partial\Omega} u^{(2)}(v)\,(\mathscr{N}^*_{\boldsymbol{\nu}}\varphi_w)\,\mathrm{d}\sigma\\ &= \int_{\Gamma_0} q^*\,\varphi_w\,\mathrm{d}\sigma - \int_{\Gamma_1} v\,(\mathscr{N}^*_{\boldsymbol{\nu}}\varphi_w)\,\mathrm{d}\sigma\,, \quad \forall\ w\in \mathrm{L}^2(\Omega)\end{aligned} \tag{2.11}$$

and the last equality becomes meaningful, provided that $\mathscr{N}^*_{\boldsymbol{\nu}}\varphi_w\in \mathrm{L}^2(\Gamma_1)$.

We conclude Step I by noting that one needs to prove that $\mathscr{N}^*_{\boldsymbol{\nu}}\psi_w, \mathscr{N}^*_{\boldsymbol{\nu}}\varphi_w\in \mathrm{L}^2(\partial\Omega)$, preferably with a continuous dependence on $w\in \mathrm{L}^2(\Omega)$, in order to obtain a rigorous Green's formula for the control problem (2.5). In fact, for numerical reasons, it turns out that even more regularity is required, namely $\mathscr{N}^*_{\boldsymbol{\nu}}\psi_w, \mathscr{N}^*_{\boldsymbol{\nu}}\varphi_w\in \mathrm{H}^{1/2}(\partial\Omega)$, see also Remark 2.2.

**Step II: Neumann regularity for $\psi_w$ and $\varphi_w$.** Due to (A1) and (A2), the following boundary regularity holds.

**Proposition 2.1.** *Let $w\in \mathrm{L}^2(\Omega)$ and let $\psi_w,\varphi_w\in \mathrm{H}^1_0(\Omega)$ be the unique weak solutions to problems (2.8) and (2.10), respectively. Then $\mathscr{N}^*_{\boldsymbol{\nu}}\psi_w, \mathscr{N}^*_{\boldsymbol{\nu}}\varphi_w\in \mathrm{H}^{1/2}(\partial\Omega)$ and the following estimate holds*

$$\exists\ c>0: \quad \|\mathscr{N}^*_{\boldsymbol{\nu}}\psi_w\|_{\mathrm{H}^{1/2}(\partial\Omega)} + \|\mathscr{N}^*_{\boldsymbol{\nu}}\varphi_w\|_{\mathrm{H}^{1/2}(\partial\Omega)} \le c\,\|w\|_{\mathrm{L}^2(\Omega)}\,.$$

*Proof.* Let us deal with $\psi_w$ only, since the case of $\varphi_w$ follows by similar regularity arguments. Note that according to Assumptions (A1) and (A2), and the local elliptic regularity, see Gilbarg and Trudinger ([17], Thm. 8.8), it follows that $\psi_w\in \mathrm{H}^2_{\mathrm{loc}}(\Omega_\varepsilon)$. In particular, $\psi_w\big|_\gamma\in \mathrm{H}^{3/2}(\gamma)$, where $\gamma := \big\{\mathbf{x}\in\overline{\Omega}_\varepsilon\ \big|\ \mathrm{dist}(\mathbf{x},\partial\Omega)=\varepsilon'\big\}$ for a sufficiently small $\varepsilon'>0$ for which $\Omega_{\varepsilon'}\subset\Omega$ and $\overline{\Omega}\setminus\overline{\Omega}_{\varepsilon'}$ is a $\mathrm{C}^2$-domain, and the following estimate holds

$$\exists\ c_1>0: \quad \|\psi_w\big|_\gamma\|_{\mathrm{H}^{3/2}(\gamma)} \le c_1\,\|w\|_{\mathrm{L}^2(\Omega)}\,.$$

According to Marschall ([36], Thm. 2), there exists an extension of $\psi_w\in \mathrm{H}^2_{\mathrm{loc}}(\Omega_\varepsilon)$, say $\widetilde{\psi}\in \mathrm{H}^2(\Omega_{\varepsilon'})$, such that $\widetilde{\psi}\big|_\gamma = \psi_w\big|_\gamma$ and the following relation holds

$$\exists\ c_2>0: \quad \|\widetilde{\psi}\|_{\mathrm{H}^2(\Omega_{\varepsilon'})} \le c_2\,\|\psi_w\big|_\gamma\|_{\mathrm{H}^{3/2}(\gamma)}\,.$$

We are now in a position to apply the global elliptic regularity result of Gilbarg and Trudinger ([17], Thm. 8.12) to obtain that $\psi_w \in \mathrm{H}^2(\Omega_{\varepsilon'})$ and the following estimate holds

$$\exists\, c_3 > 0 : \quad \|\psi_w\|_{\mathrm{H}^2(\Omega_{\varepsilon'})} \leq c_3 \, \|w\|_{\mathrm{L}^2(\Omega)} \,. \tag{2.12}$$

The claim is obtained immediately from the properties of the trace operator, see again Marschall ([36], Thm. 2), and estimate (2.12).

□

**Remark 2.2.** It is important to mention that, on the one hand, in order for relation (2.9) to be well-defined, it is sufficient that $\mathscr{N}_{\boldsymbol{\nu}}^* \psi_w \in \mathrm{L}^2(\partial\Omega)$, hence the $\mathrm{H}^{3/2+\delta}$ regularity of $\psi_w$, instead of the $\mathrm{H}^2$ regularity, in a vicinity of the boundary for the solution to problem (2.8) would be sufficient. On the other hand, the algorithm proposed in Section 3.3 requires precisely the regularity obtained by Proposition 2.1, see relation (3.26), and therefore this regularity is imperatively needed.

**Step III: Very weak solutions to and well-posedness of problems (2.4) and (2.5).** Based on Steps I and II, we are now able to introduce rigorously the following notion of very weak solutions to problems (2.4) and (2.5), respectively.

**Definition 2.3.** Consider $u^* \in \mathrm{H}^{1/2}(\Gamma_0)$ and $v \in \mathrm{L}^2(\Omega)$, and let Assumptions (A1) and (A2) hold true. We call $u^{(1)}(v) \in \mathrm{L}^2(\Omega)$ a very weak solution to problem (2.4) if

$$\int_\Omega u^{(1)}(v)\, w \, \mathrm{d}\mathbf{x} = -\int_{\Gamma_0} u^* \, (\mathscr{N}_{\boldsymbol{\nu}}^* \psi_w) \, \mathrm{d}\sigma - \int_{\Gamma_1} v \, (\mathscr{N}_{\boldsymbol{\nu}}^* \psi_w) \, \mathrm{d}\sigma \,, \quad \forall\, w \in \mathrm{L}^2(\Omega) \,, \tag{2.13}$$

where $\psi_w \in \mathrm{H}_0^1$ is the weak solution to problem (2.8).
Furthermore, problem (2.4) is called well-posed if it admits a unique very weak solution $u^{(1)}(v) \in \mathrm{L}^2(\Omega)$ and the following estimate holds

$$\exists\, C > 0 : \quad \|u^{(1)}(v)\|_{\mathrm{L}^2(\Omega)} \leq C \left( \|u^*\|_{\mathrm{L}^2(\Gamma_0)} + \|v\|_{\mathrm{L}^2(\Gamma_1)} \right) .$$

**Definition 2.4.** Consider $q^* \in \mathrm{H}^{-1/2}(\Gamma_0)$ and $v \in \mathrm{L}^2(\Omega)$, and let Assumptions (A1) and (A2) hold true. We call $u^{(2)}(v) \in \mathrm{L}^2(\Omega)$ a very weak solution to problem (2.5) if

$$\int_\Omega u^{(2)}(v)\, w \, \mathrm{d}\mathbf{x} = \int_{\Gamma_0} q^* \, \varphi_w \, \mathrm{d}\sigma - \int_{\Gamma_1} v \, (\mathscr{N}_{\boldsymbol{\nu}}^* \varphi_w) \, \mathrm{d}\sigma \,, \quad \forall\, w \in \mathrm{L}^2(\Omega) \,, \tag{2.14}$$

where $\varphi_w \in \mathrm{H}^1(\Omega)$ is the solution to problem (2.10).
Furthermore, problem (2.5) is called well-posed if it admits a unique very weak solution $u^{(2)}(v) \in \mathrm{L}^2(\Omega)$ and the following estimate holds

$$\exists\, C > 0 : \quad \|u^{(2)}(v)\|_{\mathrm{L}^2(\Omega)} \leq C \left( \|q^*\|_{\mathrm{H}^{-1/2}(\Gamma_0)} + \|v\|_{\mathrm{L}^2(\Gamma_1)} \right) .$$

Note that both notions of solutions (2.13) and (2.14) given by Definitions 2.3 and 2.4, respectively, are well-defined according to Proposition 2.1.

We are now in a position to prove that problems (2.4) and (2.5) are well-posed in the sense of Definitions 2.3 and 2.4, respectively.

**Proposition 2.5.** *Consider $u^* \in \mathrm{H}^{1/2}(\Gamma_0)$, $q^* \in \mathrm{H}^{-1/2}(\Gamma_0)$ and $v \in \mathrm{L}^2(\Omega)$, and let Assumptions* (A1) *and* (A2) *hold true. Then problems* (2.4) *and* (2.5) *are well-posed.*

*Proof.* We deal with the proof of well-posedness of problem (2.4) only, with the mention that problem (2.5) is treated in a similar manner. To do so, consider the following functional

$$G : \mathrm{L}^2(\Omega) \longrightarrow \mathbb{R}\,, \quad G(w) := -\int_{\Gamma_0} u^* \left(\mathscr{N}_{\boldsymbol{\nu}}^* \psi_w\right) \mathrm{d}\sigma - \int_{\Gamma_1} v \left(\mathscr{N}_{\boldsymbol{\nu}}^* \psi_w\right) \mathrm{d}\sigma\,, \tag{2.15}$$

where $\psi_w \in \mathrm{H}_0^1(\Omega)$ is the weak solution to problem (2.8) with $w \in \mathrm{L}^2(\Omega)$. By applying the triangle and Cauchy–Schwarz inequalities to the definition of functional (2.15) and then using Proposition 2.1, the following estimate is obtained

$$\begin{aligned} |G(w)| &\leq \|u^*\|_{\mathrm{L}^2(\Gamma_0)} \|\mathscr{N}_{\boldsymbol{\nu}}^* \psi_w\|_{\mathrm{L}^2(\Gamma_0)} + \|v\|_{\mathrm{L}^2(\Gamma_1)} \|\mathscr{N}_{\boldsymbol{\nu}}^* \psi_w\|_{\mathrm{L}^2(\Gamma_1)}, \\ &\leq C \left(\|u^*\|_{\mathrm{L}^2(\Gamma_0)} + \|v\|_{\mathrm{L}^2(\Gamma_1)}\right) \|w\|_{\mathrm{L}^2(\Omega)}\,, \quad \forall\ w \in \mathrm{L}^2(\Omega)\,. \end{aligned}$$

Consequently, it follows that $G$ is a bounded linear functional in $\mathrm{L}^2(\Omega)$ and hence the claim is a direct consequence of the Riesz representation theorem. □

We conclude this section by justifying and clarifying Assumption (A4) made in Section 2.1. In fact, the question to be addressed is the following: Is it reasonable to assume that given the observed Cauchy data $\left(u^*, q^*\right) \in \mathrm{H}^{1/2}(\Gamma_0) \times \mathrm{H}^{-1/2}(\Gamma_0)$, there exists a Dirichlet data $v \in \mathrm{L}^2(\Gamma_1)$ compatible with $\left(u^*, q^*\right)$? Here, by compatible we mean, in a rigorous manner, that $u^{(1)}(v) = u^{(2)}(v)$ in $\mathrm{L}^2(\Omega)$. The answer to this question is affirmative in the following sense.

**Proposition 2.6.** *Consider $u^* \in \mathrm{H}^{1/2}(\Gamma_0)$ and $v \in \mathrm{L}^2(\Gamma_1)$. Let Assumptions* (A1) *and* (A2) *hold true, and $u^{(1)}(v) \in \mathrm{L}^2(\Omega)$ be the very weak solution to problem* (2.4)*. Then $q^* := \mathscr{N}_{\boldsymbol{\nu}} u^{(1)}(v)\big|_{\Gamma_0} \in \mathrm{H}^{-1/2}(\Gamma_0)$. In particular, $u^{(1)}(v) = u^{(2)}(v)$.*

*Proof.* Since $\overline{\Gamma}_0 \cap \overline{\Gamma}_1 = \varnothing$, there exists $\varepsilon > 0$ such that $\operatorname{dist}(\Gamma_0, \Gamma_1) > \varepsilon$ and Assumptions (A1) and (A2) hold. Define $\Omega_\varepsilon^0 := \left\{\mathbf{x} \in \Omega \;\middle|\; \operatorname{dist}(\mathbf{x}, \Gamma_0) < \varepsilon/3\right\}$ and $\Gamma_{1,\varepsilon} := \partial\Omega_\varepsilon^0 \setminus \Gamma_0$. According to Agmon ([2], Thm. 6.2), it follows that $u^{(1)}(v) \in \mathrm{H}^1_{\mathrm{loc}}(\Omega_\varepsilon^0)$ and hence $u^{(1)}(v)\big|_{\Gamma_{1,\varepsilon}} \in \mathrm{H}^{1/2}(\Gamma_{1,\varepsilon})$. Consequently, $u := u^{(1)}(v)\big|_{\Omega_\varepsilon^0}$ is the unique weak solution to the following problem

$$\mathscr{L} u = 0 \ \text{ in } \Omega_\varepsilon^0\,, \quad u = u^* \ \text{ on } \Gamma_0\,, \quad u = u^{(1)}(v)\big|_{\Gamma_{1,\varepsilon}} \ \text{ on } \Gamma_{1,\varepsilon}$$

and hence $q^* := \mathscr{N}_{\boldsymbol{\nu}} u\big|_{\Gamma_0} \in \mathrm{H}^{-1/2}(\Gamma_0)$. □

## 3. Variational formulation

### 3.1. Reformulation of the Cauchy problem

By applying the superposition principle to direct problems (2.4) and (2.5), it follows that finding a solution to the Cauchy problem (2.1) and (2.3) is equivalent to solving the following *control problem*

$$\left|\begin{array}{l} \text{Given } u^* \in \mathrm{H}^{1/2}(\Gamma_0) \text{ and } q^* \in \mathrm{H}^{-1/2}(\Gamma_0)\,, \text{ find } v \in \mathrm{L}^2(\Gamma_1) \text{ such that} \\ \qquad\qquad u^{(1)}(v) = u^{(2)}(v)\,, \end{array}\right. \tag{3.1}$$

where $u^{(j)}(v) \in \mathrm{L}^2(\Omega)$, $j = 1, 2$, are the unique very weak solutions to direct problems (2.4) and (2.5), respectively. Moreover, the control problem (3.1) is further reformulated *via* the following functional

$$J : \mathrm{L}^2(\Gamma_1) \longrightarrow [0, \infty)\,, \qquad J(v) = \frac{1}{2} \|u^{(1)}(v) - u^{(2)}(v)\|^2_{\mathrm{L}^2(\Omega)} \tag{3.2}$$

in the form of a *minimisation problem*

$$\left|\begin{array}{l}\text{Given } u^* \in \mathrm{H}^{1/2}(\Gamma_0) \text{ and } q^* \in \mathrm{H}^{-1/2}(\Gamma_0)\,, \text{ find } v^* \in \mathrm{L}^2(\Gamma_1) \text{ such that} \\ \qquad\qquad v^* = \underset{v\in \mathrm{L}^2(\Gamma_1)}{\arg\min}\, J(v)\,.\end{array}\right. \tag{3.3}$$

Consequently, we focus on the latter problem henceforth.

### 3.2. Convexity of functional (3.2). Fréchet derivative formula

**Theorem 3.1** (Convexity of functional (3.2). Fréchet derivative formula)**.** *The functional defined by* (3.2) *is strictly convex. Moreover, the following Fréchet derivative formula holds*

$$J'(v)[h] = -\int_{\Gamma_1} \left[\mathscr{N}^*_{\mathbf{v}}\big(\psi^{(1)}(v) + \psi^{(2)}(v)\big)\right] h \,\mathrm{d}\sigma\,, \quad \forall\, h \in \mathrm{L}^2(\Gamma_1)\,, \quad \forall\, v \in \mathrm{L}^2(\Gamma_1)\,, \tag{3.4}$$

*where* $\psi^{(1)}(v) := \psi^{(1)}_{u^{(1)}(v)-u^{(2)}(v)}$ *and* $\psi^{(2)}(v) := \psi^{(2)}_{u^{(2)}(v)-u^{(1)}(v)}$ *are the unique very weak solutions to the following adjoint problems*

$$\mathscr{L}^*\psi^{(1)}(v) = u^{(1)}(v) - u^{(2)}(v) \quad \text{in } \Omega\,, \quad \psi^{(1)}(v) = 0 \quad \text{on } \Gamma_0\,, \quad \psi^{(1)}(v) = 0 \quad \text{on } \Gamma_1 \tag{3.5}$$

*and*

$$\mathscr{L}^*\psi^{(2)}(v) = u^{(2)}(v) - u^{(1)}(v) \quad \text{in } \Omega\,, \quad \mathscr{N}^*_{\mathbf{v}}\psi^{(2)}(v) = 0 \quad \text{on } \Gamma_0\,, \quad \psi^{(2)}(v) = 0 \quad \text{on } \Gamma_1\,. \tag{3.6}$$

*Proof.* For any arbitrary but fixed $v \in \mathrm{L}^2(\Gamma_1)$, we let $h \in \mathrm{L}^2(\Gamma_1)$ be arbitrary. After some computations and suitable rearrangements of the terms involved therein, the following expression is obtained

$$\begin{aligned} J(v+h) - J(v) = {} & \frac{1}{2}\,\|u^{(1)}(v+h) - u^{(1)}(v)\|^2_{\mathrm{L}^2(\Omega)} + \frac{1}{2}\,\|u^{(2)}(v+h) - u^{(2)}(v)\|^2_{\mathrm{L}^2(\Omega)}, \\ & - \langle u^{(1)}(v+h) - u^{(1)}(v), u^{(2)}(v+h) - u^{(2)}(v)\rangle_{\mathrm{L}^2(\Omega)}, \\ & + \langle u^{(1)}(v+h) - u^{(1)}(v), u^{(1)}(v) - u^{(2)}(v)\rangle_{\mathrm{L}^2(\Omega)}, \\ & + \langle u^{(2)}(v+h) - u^{(2)}(v), u^{(2)}(v) - u^{(1)}(v)\rangle_{\mathrm{L}^2(\Omega)}\,. \end{aligned} \tag{3.7}$$

By applying the superposition principle to the well-posed problems (2.4) and (2.5) with the Dirichlet boundary controls $v \in \mathrm{L}^2(\Gamma_1)$ and $v + h \in \mathrm{L}^2(\Gamma_1)$, respectively, one obtains that

$$w^{(\ell)}(h) := u^{(\ell)}(v+h) - u^{(\ell)}(v) \in \mathrm{L}^2(\Omega)\,, \quad \forall\, h \in \mathrm{L}^2(\Gamma_1)\,, \quad \ell = 1, 2,$$

are the unique very weak solutions to the well-posed boundary value problems, see Proposition 2.5,

$$\mathscr{L}w^{(1)}(h) = 0 \ \text{ in } \Omega\,, \quad w^{(1)}(h) = 0 \ \text{ on } \Gamma_0\,, \quad w^{(1)}(h) = h \ \text{ on } \Gamma_1\,, \quad \forall\, h \in \mathrm{L}^2(\Gamma_1) \tag{3.8}$$

and

$$\mathscr{L}w^{(2)}(h) = 0 \ \text{ in } \Omega\,, \quad \mathscr{N}_{\mathbf{v}}w^{(2)}(h) = 0 \ \text{ on } \Gamma_0\,, \quad w^{(2)}(h) = h \ \text{ on } \Gamma_1\,, \quad \forall\, h \in \mathrm{L}^2(\Gamma_1)\,, \tag{3.9}$$

respectively. Since problems (3.8) and (3.9) are stable, it follows that

$$\exists\, c_\ell > 0: \quad \|w^{(\ell)}(h)\|_{\mathrm{L}^2(\Omega)} \leq c_\ell\, \|h\|_{\mathrm{L}^2(\Gamma_1)}\,, \quad \forall\, h \in \mathrm{L}^2(\Gamma_1)\,, \quad \ell = 1, 2,$$

and hence the following estimates are obtained

$$\|u^{(\ell)}(v+h) - u^{(\ell)}(v)\|^2_{\mathrm{L}^2(\Omega)} = o\big(\|h\|_{\mathrm{L}^2(\Gamma_1)}\big)\,, \quad \forall\, h \in \mathrm{L}^2(\Gamma_1)\,, \quad \ell = 1, 2. \tag{3.10}$$

Further, by applying the Cauchy–Schwarz inequality to the term $\langle u^{(1)}(v+h)-u^{(1)}(v), u^{(2)}(v+h)-u^{(2)}(v)\rangle_{\mathrm{L}^2(\Omega)}$ and using estimates (3.10), one obtains

$$|\langle u^{(1)}(v+h)-u^{(1)}(v), u^{(2)}(v+h)-u^{(2)}(v)\rangle_{\mathrm{L}^2(\Omega)}| = o\big(\|h\|_{\mathrm{L}^2(\Gamma_1)}\big)\,, \quad \forall\, h\in \mathrm{L}^2(\Gamma_1)\,. \tag{3.11}$$

Consider now the adjoint problem to problem (3.8) with $h=v$ as given by relation (3.5). We note that the adjoint problem (3.5) admits a unique weak solution $\psi^{(1)}(v)\in \mathrm{H}^2(\Omega)$ since $u^{(1)}(v)-u^{(2)}(v)\in \mathrm{L}^2(\Omega)$. By setting $\psi_w=\psi^{(1)}(v)$ in the variational formulation (2.13) for the very weak solutions $u^{(1)}(v+h)$ and $u^{(1)}(v)$, respectively, and then subtracting these expressions, the following estimate is obtained

$$\langle u^{(1)}(v+h)-u^{(1)}(v), u^{(1)}(v)-u^{(2)}(v)\rangle_{\mathrm{L}^2(\Omega)} = -\int_{\Gamma_1}\big(\mathscr{N}_{\boldsymbol{\nu}}^*\psi^{(1)}(v)\big)\,h\,\mathrm{d}\sigma\,, \quad \forall\, h\in \mathrm{L}^2(\Gamma_1)\,. \tag{3.12}$$

If we consider the adjoint problem (3.6) to problem (3.9) with $h=v$ and account for the fact that $u^{(2)}(v)-u^{(1)}(v)\in \mathrm{L}^2(\Omega)$, it follows that the adjoint problem (3.6) also admits a unique weak solution $\psi^{(2)}(v)\in \mathrm{H}^2(\Omega)$. Proceeding analogously to the proof of estimate (3.12), however for $\varphi_w=\psi^{(2)}(v)$ in the variational formulation (2.14) for the very weak solutions $u^{(2)}(v+h)$ and $u^{(2)}(v)$, respectively, the following estimate is retrieved

$$\langle u^{(2)}(v+h)-u^{(2)}(v), u^{(2)}(v)-u^{(1)}(v)\rangle_{\mathrm{L}^2(\Omega)} = -\int_{\Gamma_1}\big(\mathscr{N}_{\boldsymbol{\nu}}^*\psi^{(2)}(v)\big)\,h\,\mathrm{d}\sigma\,, \quad \forall\, h\in \mathrm{L}^2(\Gamma_1)\,. \tag{3.13}$$

Expression (3.7) and estimates (3.10)–(3.13) imply that

$$J(v+h)-J(v) = -\int_{\Gamma_1}\big[\mathscr{N}_{\boldsymbol{\nu}}^*\big(\psi^{(1)}(v)+\psi^{(2)}(v)\big)\big]\,h\,\mathrm{d}\sigma + o\big(\|h\|_{\mathrm{L}^2(\Gamma_1)}\big)\,, \quad \forall\, h\in \mathrm{L}^2(\Gamma_1)\,,$$

hence functional $J$ given by (3.2) is Fréchet differentiable in $\mathrm{L}^2(\Gamma_1)$ and the following relation holds

$$J'(v)[h] = -\int_{\Gamma_1}\big[\mathscr{N}_{\boldsymbol{\nu}}^*\big(\psi^{(1)}(v)+\psi^{(2)}(v)\big)\big]\,h\,\mathrm{d}\sigma\,, \quad \forall\, v\in \mathrm{L}^2(\Gamma_1)\,, \quad \forall\, h\in \mathrm{L}^2(\Gamma_1)\,. \tag{3.14}$$

The linearity of direct problems (2.4) and (3.8) on the one hand and that of direct problems (2.5) and (3.9) on the other hand imply that

$$u^{(\ell)}(v) = u^{(\ell)}(0)+w^{(\ell)}(v)\,, \quad \forall\, v\in \mathrm{L}^2(\Gamma_1)\,, \quad \ell=1,2, \tag{3.15}$$

where $u^{(\ell)}(0)$, $\ell=1,2$, are the very weak solutions of direct problems (2.4) and (2.5), respectively, with $v=0$. A direct consequence of relation (3.15) is the following natural splitting

$$u^{(1)}(v)-u^{(2)}(v) = \big(u^{(1)}(0)-u^{(2)}(0)\big)+\big(w^{(1)}(v)-w^{(2)}(v)\big)\,, \quad \forall\, v\in \mathrm{L}^2(\Gamma_1)\,. \tag{3.16}$$

Consider now the adjoint problems to problems (3.8) and (3.9) with $h=v$, namely

$$\mathscr{L}^*\varphi^{(1)}(v) = w^{(1)}(v)-w^{(2)}(v) \ \text{ in } \Omega\,, \quad \varphi^{(1)}(v)=0 \ \text{ on } \Gamma_0\,, \quad \varphi^{(1)}(v)=0 \ \text{ on } \Gamma_1 \tag{3.17}$$

and

$$\mathscr{L}^*\varphi^{(2)}(v) = w^{(2)}(v)-w^{(1)}(v) \ \text{ in } \Omega\,, \quad \mathscr{N}_{\boldsymbol{\nu}}^*\varphi^{(2)}(v)=0 \ \text{ on } \Gamma_0\,, \quad \varphi^{(2)}(v)=0 \ \text{ on } \Gamma_1\,, \tag{3.18}$$

respectively, where $\varphi^{(1)}(v) := \varphi^{(1)}_{w^{(1)}(v)-w^{(2)}(v)}$ and $\varphi^{(2)}(v) := \varphi^{(2)}_{w^{(2)}(v)-w^{(1)}(v)}$.

Expression (3.14) and the linearity of Neumann conditions for the adjoint problems (3.6) and (3.18) yield

$$\begin{aligned} J'(v+h_2)[h_1] = J'(v)[h_1] - \int_{\Gamma_1}\big[\mathscr{N}_{\boldsymbol{\nu}}^*\big(\varphi^{(1)}(h_2)+\varphi^{(2)}(h_2)\big)\big]\,h_1\,\mathrm{d}\sigma\,,\\ \forall\, v\in \mathrm{L}^2(\Gamma_1)\,, \quad \forall\, h_\ell\in \mathrm{L}^2(\Gamma_1)\,, \quad \ell=1,2. \end{aligned} \tag{3.19}$$

Clearly, the second term in (3.19) is also linear with respect to $h_2 \in \mathrm{L}^2(\Gamma_1)$ by the linearity of Neumann conditions for the adjoint problems (3.6) and (3.18). Therefore, $J$ is twice Fréchet differentiable and the following expression is obtained

$$J''(v)[h_1,h_2] = -\int_{\Gamma_1} \left[\mathscr{N}_{\boldsymbol{\nu}}^*\left(\varphi^{(1)}(h_2)+\varphi^{(2)}(h_2)\right)\right] h_1 \,\mathrm{d}\sigma\,, \quad \forall\, v \in \mathrm{L}^2(\Gamma_1)\,, \quad \forall\, h_\ell \in \mathrm{L}^2(\Gamma_1)\,, \quad \ell = 1,2. \tag{3.20}$$

Green's formulae for problems (3.8) and (3.17) on the one hand (*i.e.* Def. 2.3), and problems (3.9) and (3.18) on the other hand (*i.e.* Def. 2.4) for $v = h$ read as

$$\int_\Omega w^{(1)}(h)\left(w^{(1)}(h)-w^{(2)}(h)\right)\mathrm{d}\mathbf{x} = -\int_{\Gamma_1}\left(\mathscr{N}_{\boldsymbol{\nu}}^*\varphi^{(1)}(h)\right) h\,\mathrm{d}\sigma\,, \quad \forall\, h\in\mathrm{L}^2(\Omega) \tag{3.21a}$$

and

$$\int_\Omega w^{(2)}(h)\left(w^{(2)}(h)-w^{(1)}(h)\right)\mathrm{d}\mathbf{x} = -\int_{\Gamma_1}\left(\mathscr{N}_{\boldsymbol{\nu}}^*\varphi^{(2)}(h)\right) h\,\mathrm{d}\sigma\,, \quad \forall\, h\in\mathrm{L}^2(\Omega)\,. \tag{3.21b}$$

Summing up relations (3.21a)–(3.21b) and using (3.20) with $h := h_1 = h_2$, one obtains

$$J''(v)[h,h] = \|w^{(1)}(h)-w^{(2)}(h)\|^2_{\mathrm{L}^2(\Omega)}\,, \quad \forall\, v\in\mathrm{L}^2(\Gamma_1)\,, \quad \forall\, h\in\mathrm{L}^2(\Gamma_1) \tag{3.22}$$

and this shows the convexity of functional $J$.

Assume now that $J''(v)[h,h] = 0$ for some $h \in \mathrm{L}^2(\Gamma_1)$, hence $w^{(1)}(h) = w^{(2)}(h)$ in $\mathrm{L}^2(\Omega)$ by (3.22). Consequently, $w(h) := w^{(1)}(h) = w^{(2)}(h) \in \mathrm{L}^2(\Omega)$ satisfies, in a very weak sense, the Cauchy problem

$$\mathscr{L}w(h) = 0 \ \text{ in } \Omega\,, \quad w(h) = 0 \ \text{ on } \Gamma_0\,, \quad \mathscr{N}_{\boldsymbol{\nu}}w(h) = 0 \ \text{ on } \Gamma_0$$

and, according to a uniqueness theorem of the Cauchy problem for the Laplace–Beltrami equation, it follows that $w(h) \equiv 0$ in $\overline{\Omega}$. Therefore, $w(h)\big|_{\Gamma_1} = w^{(\ell)}(h)\big|_{\Gamma_1} = h = 0$, $\ell = 1,2$, hence functional $J$ is strictly convex. □

**Remark 3.2.** (i) By setting $d(v) := \mathscr{N}_{\boldsymbol{\nu}}^*\left(\psi^{(1)}(v)+\psi^{(2)}(v)\right)\big|_{\Gamma_1}$, relation (3.14) becomes

$$J'(v)[h] = -\int_{\Gamma_1} d(v)\, h\,\mathrm{d}\sigma\,, \quad \forall\, h\in\mathrm{L}^2(\Gamma_1)\,, \quad \forall\, v\in\mathrm{L}^2(\Gamma_1)\,. \tag{3.23}$$

By the Riesz representation theorem, $J'(v) \in \mathrm{H}^{-1/2}(\Gamma_1)$ from (3.14) may be identified with the trace on $\Gamma_1$ of the solution to a suitable mixed boundary value problem and this yields the so-called *gradient descent method* (*GDM*) presented in [35].

(ii) The key idea of the algorithm proposed here is that by the crucial Proposition 2.1, it follows, in fact, that $d(v) \in \mathrm{H}^{1/2}(\Gamma_1)$ and, therefore, one can overcome the computation of the aforementioned mixed boundary value problem by considering $d(v)$ as the direction for updating the approximation of the unknown Dirichlet data on $\Gamma_1$. This procedure actually yields a simpler version of the GDM, referred to as the *weak GDM* (*wGDM*), that is also weaker than the GDM in a sense to be made more precise later.

### 3.3. Algorithm: The weak GDM (wGDM)

As a direct consequence of the Fréchet derivative (gradient) formula (3.4), the following algorithm (wGDM) is obtained:

Step 1 `Set` $k = 0$. `Choose an approximation for` $u\big|_{\Gamma_1} \in \mathrm{L}^2(\Gamma_1)$, $v_k \in \mathrm{L}^2(\Gamma_1)$.

Step 2 Solve the following direct problems

$$\mathscr{L}u^{(1)}(v_k) = 0 \ \text{ in } \Omega\,, \quad u^{(1)}(v_k) = u^* \ \text{ on } \Gamma_0\,, \quad u^{(1)}(v_k) = v_k \ \text{ on } \Gamma_1 \tag{3.24a}$$

and

$$\mathscr{L}u^{(2)}(v_k) = 0 \ \text{ in } \Omega\,, \quad \mathscr{N}_{\boldsymbol{\nu}}u^{(2)}(v_k) = q^* \ \text{ on } \Gamma_0\,, \quad u^{(2)}(v_k) = v_k \ \text{ on } \Gamma_1\,. \tag{3.24b}$$

Step 3 Solve the corresponding adjoint problems

$$\mathscr{L}^*\psi_k^{(1)} = u^{(1)}(v_k) - u^{(2)}(v_k) \ \text{ in } \Omega\,, \quad \psi_k^{(1)} = 0 \ \text{ on } \Gamma_0\,, \quad \psi_k^{(1)} = 0 \ \text{ on } \Gamma_1 \tag{3.25a}$$

and

$$\mathscr{L}^*\psi_k^{(2)} = u^{(2)}(v_k) - u^{(1)}(v_k) \ \text{ in } \Omega\,, \quad \mathscr{N}_{\boldsymbol{\nu}}^*\psi_k^{(2)} = 0 \ \text{ on } \Gamma_0\,, \quad \psi_k^{(2)} = 0 \ \text{ on } \Gamma_1 \tag{3.25b}$$

to determine the direction

$$d_k\big|_{\Gamma_1} = \mathscr{N}_{\boldsymbol{\nu}}^*\psi_k^{(1)}\big|_{\Gamma_1} + \mathscr{N}_{\boldsymbol{\nu}}^*\psi_k^{(2)}\big|_{\Gamma_1} \in \mathrm{H}^{1/2}(\Gamma_1)\,. \tag{3.26}$$

Set the approximation for $u\big|_{\Gamma_1}$ as

$$v_{k+1}\big|_{\Gamma_1} = v_k\big|_{\Gamma_1} + \gamma_k\, d_k\big|_{\Gamma_1} \in \mathrm{H}^{1/2}(\Gamma_1)\,, \tag{3.27}$$

where $\gamma_k > 0$ is a relaxation parameter.

Step 4 Set $k = k+1$. Repeat Steps $2-3$ until a prescribed stopping criterion is satisfied.

**Remark 3.3.** (i) The linearity of adjoint problems (3.5) and (3.17), and that of adjoint problems (3.6) and (3.18), in conjunction with relation (3.16), yield

$$\psi^{(\ell)}(v) = \psi^{(\ell)}(0) + \varphi^{(\ell)}(v)\,, \quad \forall\, v \in \mathrm{L}^2(\Gamma_1)\,, \quad \ell = 1, 2, \tag{3.28}$$

where $\psi^{(\ell)}(0)$, $\ell = 1, 2$, are the very weak solutions to problems (3.5) and (3.6), respectively, with $v = 0$.

(ii) Relations (3.28) and (3.4) imply that

$$\begin{aligned} J'(v) &= -\mathscr{N}_{\boldsymbol{\nu}}^*\big(\psi^{(1)}(0) + \psi^{(2)}(0)\big)\big|_{\Gamma_1} - \mathscr{N}_{\boldsymbol{\nu}}^*\big(\varphi^{(1)}(v) + \varphi^{(2)}(v)\big)\big|_{\Gamma_1} \\ &=: -d_0 - \widetilde{d}(v)\,, \quad \forall\, v \in \mathrm{L}^2(\Gamma_1)\,. \end{aligned} \tag{3.29}$$

Consequently, according to relation (3.29), the above wGDM can be modified to account for:

(a) a sole computation of the direction $d_0 \in \mathrm{H}^{1/2}(\Gamma_1)$ by solving, at the very beginning of the iterative procedure, the direct problems (2.4) and (2.5), and their corresponding adjoint problems (3.5) and (3.6) with $v = 0$;

(b) an iterative computation of the direction $\widetilde{d}(v) \in \mathrm{H}^{1/2}(\Gamma_1)$ by solving, at each iteration, the direct problems (3.8) and (3.9) with $h = v$, and their corresponding adjoint problems (3.17) and (3.18).

## 4. Convergence of the wGDM

Herein we investigate the convergence of the wGDM algorithm developed for solving the minimisation problem (3.3) and discuss the admissible range for the relaxation parameter $\gamma_k > 0$, $k \geq 0$.

**Theorem 4.1.** *Assume that the Cauchy problem (2.1) and (2.3) with $u^* \in \mathrm{H}^{1/2}(\Gamma_0)$ and $q^* \in \mathrm{H}^{-1/2}(\Gamma_0)$ admits a solution. Let $v_0 \in \mathrm{H}^{1/2}(\Gamma_1)$ be an initial approximation for the solution to minimisation problem (3.3) and $v_0^*$ be the projection of $v_0$ on the closed convex set of solutions to the minimisation problem (3.3), i.e.*

$$v_0^* := \underset{\substack{v\in \mathrm{L}^2(\Gamma_1)\\ J(v)=0}}{\arg\min} \|v - v_0\|_{\mathrm{L}^2(\Gamma_1)}.$$

*If the sequence $\{v_k\}_{k\geq 0} \subset \mathrm{H}^{1/2}(\Gamma_1)$ is generated by the wGDM algorithm (3.24)–(3.27) with $k_0 \geq 0$ and $\varepsilon > 0$ such that*

$$0 < \varepsilon \leq \gamma_k \leq (2-\varepsilon)\,\frac{\|u^{(1)}(v_k) - u^{(2)}(v_k)\|^2_{\mathrm{L}^2(\Omega)}}{\|d_k\|^2_{\mathrm{L}^2(\Gamma_1)}}\,, \quad k \geq k_0\,,$$

*then*

$$\lim_{k\to\infty} J\big(v_k\big) = 0$$

*and*

$$\lim_{k\to\infty} v_k = v_0^* \quad \textit{weakly in} \quad \mathrm{L}^2(\Gamma_1)\,.$$

*Proof.* We proceed in several steps.

**Step I.** We claim that the sequence $\{v_k\}_{k\geq 0}$ is bounded in $\mathrm{L}^2(\Gamma_1)$ and $\lim_{k\to\infty} J\big(v_k\big) = 0$. For any $h \in \mathrm{H}^{1/2}(\Gamma_1)$, it follows, from estimates (3.12), (3.13) and (3.23), that

$$\begin{aligned}
\big\langle d_k,\, h\big\rangle_{\mathrm{L}^2(\Gamma_1)} &= -J'(v_k)[h] = \int_{\Gamma_1} \big[\mathscr{N}_{\mathbf{v}}^*\big(\psi_k^{(1)} + \psi_k^{(2)}\big)\big]\, h\,\mathrm{d}\sigma \\
&= -\big\langle u^{(1)}(v_k + h) - u^{(1)}(v_k),\, u^{(1)}(v_k) - u^{(2)}(v_k)\big\rangle_{\mathrm{L}^2(\Omega)} \\
&\quad - \big\langle u^{(2)}(v_k + h) - u^{(2)}(v_k),\, u^{(2)}(v_k) - u^{(1)}(v_k)\big\rangle_{\mathrm{L}^2(\Omega)} \\
&= \big\langle u^{(2)}(v_k + h) - u^{(1)}(v_k + h) + u^{(1)}(v_k) - u^{(2)}(v_k),\, u^{(1)}(v_k) - u^{(2)}(v_k)\big\rangle_{\mathrm{L}^2(\Omega)}\,.
\end{aligned} \tag{4.1}$$

Denote $v_k^* := v_0^* - v_k$. By using the assumptions made on $\gamma_k$, $k \geq k_0$, and estimate (4.1), one obtains

$$\begin{aligned}
&\|v_{k+1}^*\|^2_{\mathrm{L}^2(\Gamma_1)} = \|v_k^* - \gamma_k d_k\|^2_{\mathrm{L}^2(\Gamma_1)} = \|v_k^*\|^2_{\mathrm{L}^2(\Gamma_1)} - 2\gamma_k\big\langle d_k,\, v_k^*\big\rangle_{\mathrm{L}^2(\Gamma_1)} + \gamma_k^2\|d_k\|^2_{\mathrm{L}^2(\Gamma_1)} \\
&= \|v_k^*\|^2_{\mathrm{L}^2(\Gamma_1)} - 2\gamma_k\big\langle u^{(2)}(v_0^*) - u^{(1)}(v_0^*) + u^{(1)}(v_k) - u^{(2)}(v_k),\, u^{(1)}(v_k) - u^{(2)}(v_k)\big\rangle_{\mathrm{L}^2(\Omega)} \\
&+ \gamma_k^2\|d_k\|^2_{\mathrm{L}^2(\Gamma_1)} = \|v_k^*\|^2_{\mathrm{L}^2(\Gamma_1)} - 2\gamma_k\|u^{(1)}(v_k) - u^{(2)}(v_k)\|^2_{\mathrm{L}^2(\Omega)} + \gamma_k^2\|d_k\|^2_{\mathrm{L}^2(\Gamma_1)} \\
&\leq \|v_k^*\|^2_{\mathrm{L}^2(\Gamma_1)} - \gamma_k\varepsilon\|u^{(1)}(v_k) - u^{(2)}(v_k)\|^2_{\mathrm{L}^2(\Omega)} \leq \|v_k^*\|^2_{\mathrm{L}^2(\Gamma_1)} - \varepsilon^2\|u^{(1)}(v_k) - u^{(2)}(v_k)\|^2_{\mathrm{L}^2(\Omega)} \\
&= \|v_k^*\|^2_{\mathrm{L}^2(\Gamma_1)} - 2\varepsilon^2 J(v_k)\,, \quad k \geq k_0\,,
\end{aligned}$$

and this proves the claim.

**Step II.** We show that if $\lim_{n\to\infty} v_{k_n} = v$ weakly in $\mathrm{L}^2(\Gamma_1)$, then $v \in \mathrm{L}^2(\Gamma_1)$ is a solution to minimisation problem (3.3), *i.e.* $J(v) = 0$.

By the Banach–Saks Theorem [43], there exists $\{v_{k_{n_\ell}}\}_{\ell\geq 0} \subset \{v_{k_n}\}_{n\geq 0}$ such that

$$\lim_{N\to\infty} \left\| \frac{1}{N}\sum_{\ell\geq N} v_{k_{n_\ell}} - v \right\|_{\mathrm{L}^2(\Gamma_1)} = 0\,.$$

The convexity of functional $J$ and the result proved at Step I imply that

$$J\big(v\big) = \lim_{N\to\infty} J\bigg(\frac{1}{N}\sum_{\ell\geq N} v_{k_{n_\ell}}\bigg) \leq \limsup_{N\to\infty} \frac{1}{N}\sum_{\ell\geq N} J\big(v_{k_{n_\ell}}\big) = 0\,.$$

**Step III.** We prove by induction that $\big\langle v_k - v_0^*, w - v_0^*\big\rangle_{\mathrm{L}^2(\Gamma_1)} \leq 0$, $k\geq 0$, for any $w\in \mathrm{L}^2(\Gamma_1)$ such that $J(w)=0$.

For $k=0$, the claim follows from the variational characterisation of $v_0^*$.
We further assume that the claim holds for some $k\geq 0$. By employing once again estimate (4.1) and the superposition principle for problems (2.4) and (2.5), it follows that

$$\begin{aligned}
&\big\langle v_{k+1} - v_0^*, w - v_0^*\big\rangle_{\mathrm{L}^2(\Gamma_1)},\\
&= \big\langle v_k - v_0^*, w - v_0^*, \big\rangle_{\mathrm{L}^2(\Gamma_1)} + \gamma_k \big\langle d_k, w - v_0^*\big\rangle_{\mathrm{L}^2(\Gamma_1)}, \leq \gamma_k \big\langle d_k, w - v_0^*\big\rangle_{\mathrm{L}^2(\Gamma_1)},\\
&= \gamma_k \big\langle u^{(2)}(v_k + w - v_0^*) - u^{(1)}(v_k + w - v_0^*) + u^{(1)}(v_k) - u^{(2)}(v_k),\, u^{(1)}(v_k) - u^{(2)}(v_k)\big\rangle_{\mathrm{L}^2(\Omega)},\\
&= \gamma_k \big\langle u^{(2)}(w - v_0^*) - u^{(1)}(w - v_0^*),\, u^{(1)}(v_k) - u^{(2)}(v_k)\big\rangle_{\mathrm{L}^2(\Omega)} = 0\,, \quad \forall\ w\in \mathrm{L}^2(\Gamma_1):\ J(w)=0,
\end{aligned}$$

since $J(w - v_0^*) = 0$. Consequently, the claim also holds for $k+1$.
**Step IV.** We finally show that $\lim\limits_{k\to\infty} v_k = v_0^*$ weakly in $\mathrm{L}^2(\Gamma_1)$.

According to Step I, $\big\{v_k\big\}_{k\geq 0}$ is weakly relatively compact in $\mathrm{L}^2(\Gamma_1)$. Hence it is sufficient to show that any accumulation point of $\big\{v_k\big\}_{k\geq 0}$ in the weak topology of $\mathrm{L}^2(\Gamma_1)$ coincides with $v_0^*$. However, the latter is just a consequence of Steps II and III.

□

**Remark 4.2.** It can also be proved that if, in addition, the sequence $\big\{\gamma_k\big\}_{k\geq 0}$ defined above satisfies

$$\exists\ k_0\geq 0: \quad \gamma_k \leq \frac{2}{\|A^*A\|}\,, \quad k\geq k_0\,,$$

where $A : \mathrm{H}^{1/2}(\Gamma_1) \longrightarrow \mathrm{L}^2(\Omega)$, $A(v) := \big(u^{(2)}(v) - u^{(2)}(0)\big) - \big(u^{(1)}(v) - u^{(1)}(0)\big)$, then

$$\lim_{k\to\infty} \|v_k - v_0^*\|_{\mathrm{H}^{1/2}(\Gamma_1)} = 0\,.$$

**Remark 4.3.** For the wGDM algorithm, there are two options for selecting the optimal value of the relaxation parameter $\gamma_k$, $k\geq 0$, see Step III, namely

(i) by minimising $J\big(v_{k+1}\big)$ at each iteration $k\geq 0$, *i.e.*

$$\gamma_k^{\mathrm{opt}} := \operatorname*{arg\,min}_{\gamma_k\geq 0} J\big(v_{k+1}\big) = \frac{\|d_k\|^2_{\mathrm{L}^2(\Gamma_1)}}{\|Ad_k\|^2_{\mathrm{L}^2(\Omega)}}\,, \quad k\geq 0\,;$$

(ii) by minimising $\big\|v_{k+1} - v_0^*\big\|_{\Gamma_1}$ at each iteration $k\geq 0$, *i.e.*

$$\widehat{\gamma}_k^{\mathrm{opt}} := \operatorname*{arg\,min}_{\gamma_k\geq 0} \big\|v_{k+1} - v_0^*\big\|_{\Gamma_1} = \frac{\|u^{(1)}(v_k) - u^{(2)}(v_k)\|^2_{\mathrm{L}^2(\Omega)}}{\|d_k\|^2_{\mathrm{L}^2(\Gamma_1)}}\,, \quad k\geq 0\,.$$

Clearly, $\gamma_k^{\mathrm{opt}} \leq \widehat{\gamma}_k^{\mathrm{opt}}$ and Theorem 4.1 is applicable for both $\gamma_k^{\mathrm{opt}}$ and $\widehat{\gamma}_k^{\mathrm{opt}}$. Hence the weak convergence of the wGDM with either $\gamma_k := \gamma_k^{\mathrm{opt}}$, $k\geq 0$, or $\gamma_k := \widehat{\gamma}_k^{\mathrm{opt}}$, $k\geq 0$, is guaranteed.

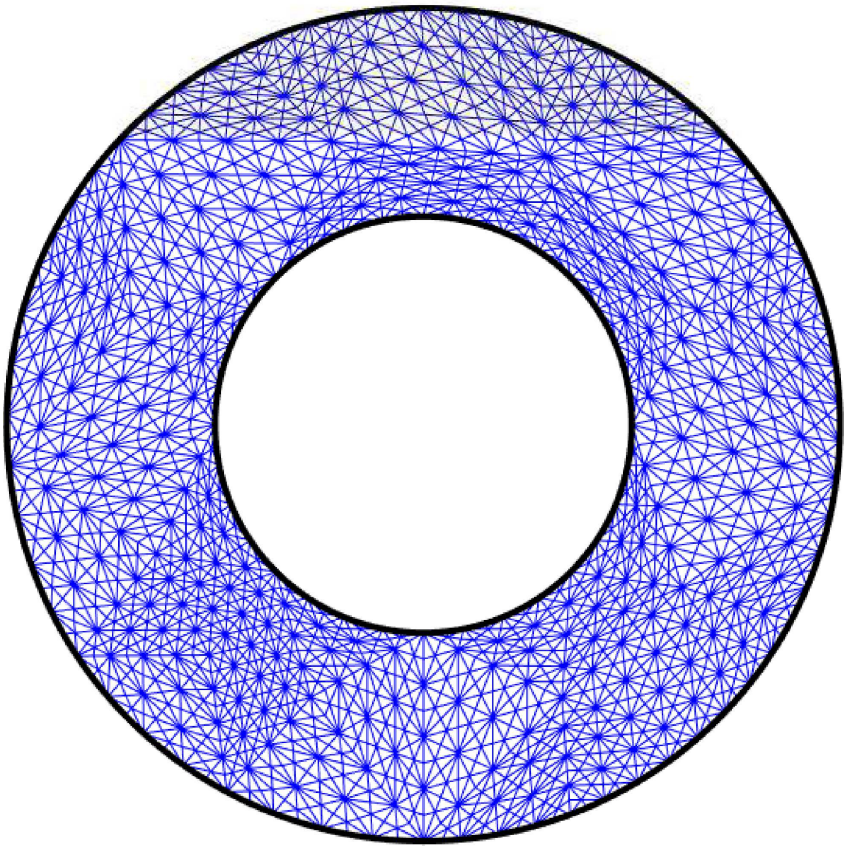

FIGURE 1. Schematic diagram of the FEM conforming triangulation $\mathcal{T}_h$ of the domain $\Omega$.

## 5. Numerical approximation: Finite element method (FEM)

Under the assumptions made in Section 2, the Cauchy problem given by (2.1) and (2.3) is approximated numerically using the FEM and this is briefly presented further.

**FEM approximation of control problems (2.4) and (2.5).** Given a doubly connected domain $\Omega \subset \mathbb{R}^2$ with a smooth boundary $\partial\Omega = \Gamma_0 \cup \Gamma_1$ such that $\varnothing \neq \Gamma_0, \Gamma_1 \subsetneq \partial\Omega$ and $\overline{\Gamma}_0 \cap \overline{\Gamma}_1 = \varnothing$, we seek for the piecewise continuous polynomial approximations to the unique very weak solution of boundary value problems (2.4) and (2.5), $u^{(j)}(v) \in \mathrm{L}^2(\Omega)$, $j = 1, 2$, respectively, *via* the FEM. To do so, the domain $\Omega$ is partitioned *via* a conforming triangulation $\mathcal{T}_h \subset \mathcal{P}(\Omega)$, see Figure 1, that is non-degenerate in the sense of Gockenbach ([18], Sect. 5.1.2) and is defined by the following properties:

(T1) $\overline{\Omega} = \bigcup_{K \in \mathcal{T}_h} K$, where $K \in \mathcal{T}_h$ is referred to as a geometric element;
(T2) $\forall\, K \in \mathcal{T}_h$, $K$ is a polyhedron such that $\mathrm{int}(K) \neq \varnothing$;
(T3) $\forall\, K_1, K_2 \in \mathcal{T}_h$: $K_1 \neq K_2$, then $\mathrm{int}(K_1) \cap \mathrm{int}(K_2) = \varnothing$;
(T4) $\forall\, K_1, K_2 \in \mathcal{T}_h$: $K_1 \neq K_2$, then $\overline{K}_1 \cap \overline{K}_2 \neq \varnothing$ is either a common vertex or a common edge for $K_1$ and $K_2$.

We note that a global measure of the FEM triangulation $\mathcal{T}_h$ is given by $h := \max_{K \in \mathcal{T}_h} h_K$, where $h_K := \max_{\mathbf{x},\mathbf{y} \in K} \|\mathbf{x}-\mathbf{y}\|_2$ denotes the diameter of a geometric element $K$.

The FEM approximation to the unique weak solution of problem (2.5) with a homogeneous boundary control $v \equiv 0$, denoted by $u^{(2)}(0) \in \mathrm{H}^1(\Omega)$, is obtained by requiring it to be second-order degree polynomials on each $K \in \mathcal{T}_h$, continuous over any two adjacent elements and satisfying a homogeneous Dirichlet boundary condition on $\Gamma_1$, namely

$$U_h^{(2)} \coloneqq \left\{ v_h \in \mathrm{C}(\overline{\Omega}) \;\middle|\; v_h|_{\Gamma_1} = 0\,; \;\; v_h|_K \in \mathbb{P}_2(K),\ \forall\ K \in \mathcal{T}_h \right\},$$

where $\mathbb{P}_2(K)$ denotes the set of second-order degree polynomials on $K$. Let $\left\{\varphi_j\right\}_{j=\overline{1,N_h}}$ be the standard Lagrange basis for the finite-dimensional space $U_h^{(2)}$, where $N_h \coloneqq \dim\left(U_h\right) < \infty$. Thus, the FEM solution $u_h^{(2)}(0) \in U_h^{(2)}$ may be expressed as

$$u_h^{(2)}(0)(\mathbf{x}) = \sum_{j=1}^{N_h} \xi_j \varphi_j(\mathbf{x})\,, \quad \mathbf{x} \in \overline{\Omega}\,,$$

where the vector $\xi \coloneqq (\xi_i)_{i=\overline{1,N_h}} \in \mathbb{R}^{N_h}$ contains the unknown values of $u_h^{(2)}(0)$ at the nodes of $\mathcal{T}_h$. These latter values are retrieved *via* a standard Galerkin approximation which yields the following homogeneous linear system of $N_h$ equations with $N_h$ unknowns

$$\mathbf{A}\xi = \mathbf{b},$$

where

$$\mathbf{A} = (A_{ij})_{i,j=\overline{1,N_h}} \in \mathbb{R}^{N_h \times N_h}, \qquad A_{ij} \coloneqq \int_\Omega (\mathbf{K}\nabla\varphi_i) \cdot \nabla\varphi_j \,\mathrm{d}\mathbf{x}, \quad i,j = \overline{1,N_h},$$

$$\mathbf{b} = (b_i)_{i=\overline{1,N_h}} \in \mathbb{R}^{N_h}, \qquad b_i \coloneqq \int_{\Gamma_0} q^* \varphi_i \,\mathrm{d}\sigma, \quad i = \overline{1,N_h}.$$

We also note that the FEM approximation to the unique weak solution of problem (2.4) with a homogeneous control $v \equiv 0$ and $u^* \equiv 0$, denoted by $u^{(1)}(0) \in \mathrm{H}^1(\Omega)$, as well as the corresponding FEM space of solutions $U_h^{(1)}$ are constructed analogously and, therefore, they are omitted here.

We further consider an arbitrary regular boundary control $v \in \mathrm{H}^{1/2}(\Gamma_1)$, extend it continuously to a function $\widetilde{v} \in \mathrm{H}^1(\Omega)$ such that $\widetilde{v}|_{\Gamma_1} = v$ and $\widetilde{v}|_{\Gamma_0} = 0$, see *e.g.* [18], and define the corresponding unique FEM solutions to problems (2.4) and (2.5), $u_h^{(j)}(v) \in \mathrm{H}^1(\Omega)$, $j = 1,2$, respectively, as

$$u_h^{(j)}(v) \coloneqq u_h^{(j)}(0) + \widetilde{v}, \quad \forall\ v \in \mathrm{H}^{1/2}(\Gamma_1), \quad j = 1,2.$$

Finally, the case of merely square-integrable boundary control $v \in \mathrm{L}^2(\Gamma_1)$ is treated by considering the $\mathrm{L}^2$–projections on the FEM solution spaces of direct problems (2.4) and (2.5), $v_h^{(j)} \in U_h^{(j)}|_{\Gamma_1}$, $j = 1,2$, respectively, defined by

$$\int_{\Gamma_1} v_h^{(j)} \varphi_h \mathrm{d}\sigma = \int_{\Gamma_1} v \varphi_h \mathrm{d}\sigma, \quad \forall\ \varphi_h \in U_h^{(j)}|_{\Gamma_1}, \quad j = 1,2. \tag{5.1}$$

Theorem 5.2 from Berggren [10] enables one the replacement of $v \in \mathrm{L}^2(\Gamma_1)$ with $v_h^{(j)} \in U_h^{(j)}\big|_{\Gamma_1}$, $j = 1,2$, and the application of the FEM yields the unique FEM solutions to problems (2.4) and (2.5), $u_h^{(j)}(v) \in \mathrm{H}^1(\Omega)$, $j = 1,2$, that approximate their corresponding unique very weak solutions, $u^{(j)}(v) \in \mathrm{L}^2(\Omega)$, $j = 1,2$.

**FEM approximation of minimisation problem (3.3).** The minimisation functional $J$ given by (3.2) is approximated, *via* the FEM non-degenerate conforming triangulation of $\Omega$, $\mathcal{T}_h$, $h > 0$, as

$$J_h : \mathrm{L}^2(\Gamma_1) \longrightarrow [0,\infty)\,, \quad J_h(v) = \frac{1}{2}\left\| u_h^{(1)}(v) - u_h^{(2)}(v) \right\|^2_{\mathrm{L}^2(\Omega)}, \tag{5.2}$$

where $u_h^{(j)}(v) \in \mathrm{H}^1(\Omega)$, $j = 1,2$, are the unique FEM solutions to direct problems (2.4) and (2.5), respectively.

**Theorem 5.1** (Convergence of the FEM approximation of minimisation problem (3.3))**.** *Consider* $J_h^* := \inf_{v\in \mathrm{L}^2(\Gamma_1)} J_h(v)$*, where* $J_h$ *is defined by* (5.2)*. Then* $\lim_{h\to 0} J_h^* = 0$.

*Let* $h>0$ *and* $v_h \in \mathrm{L}^2(\Gamma_1)$ *be the function obtained after a sufficient number of steps in the wGDM* (3.25)–(3.27) *with the FEM non-degenerate conforming triangulation* $\mathcal{T}_h$ *such that* $J_h^* \le J_h(v_h) \le J_h^* + \varepsilon_h$*, where* $\varepsilon_h \ge 0$ *and* $\lim_{h\to 0}\varepsilon_h = 0$*. If* $\{v_h\}_{h>0} \subset \mathrm{L}^2(\Gamma_1)$ *is bounded and* $v^* = \arg\min_{v\in \mathrm{L}^2(\Gamma_1)} J(v)$ *is the unique solution of minimisation problem* (3.3)*, then* $\lim_{h\to 0}\|v_h - v^*\|_{\mathrm{L}^2(\Gamma_1)} = 0$*. In particular, if* $u^{(\mathrm{ex})}$ *is the solution of the Cauchy problem* (2.1) *and* (2.3)*, then* $\lim_{h\to 0}\|u_h - u^{(\mathrm{ex})}\|_{\mathrm{L}^2(\Omega)} = 0$.

*Proof.* The convergence of the FEM approximations used for the problems (2.4) and (2.5) implies that $\lim_{h\to 0}\|u_h^{(\ell)}(v) - u^{(\ell)}(v)\|_{\mathrm{H}^1(\Omega)} = 0$, for any $v \in \mathrm{L}^2(\Gamma_1)$, $\ell = 1,2$, see Gockenbach ([18], Thm. 5.5). Therefore, it follows that

$$\lim_{h\to 0} J_h(v) = J(v), \quad \forall\, v \in \mathrm{L}^2(\Gamma_1). \tag{5.3}$$

By taking $v = v^*$ in relation (5.3) and considering the definition of $J_h^*$, one obtains that

$$\lim_{h\to 0} J_h^* \le \lim_{h\to 0} J_h(v^*) = J(v^*) = 0. \tag{5.4}$$

On accounting for the definition of $v_h$ and relations (5.3) and (5.4), it follows that

$$\begin{aligned} 0 \le J(v_h) &= \left|\left(J(v_h) - J_h(v_h)\right) + \left(J_h(v_h) - J_h^*\right) + J_h^*\right| \\ &\le \left|J(v_h) - J_h(v_h)\right| + \left|J_h(v_h) - J_h^*\right| + J_h^* \overset{h\to 0}{\longrightarrow} 0 \end{aligned}$$

and hence one obtains that $\{v_h\}_{h>0} \subset \mathrm{L}^2(\Gamma_1)$ is a minimising sequence for functional $J$. The sequence $\{v_h\}_{h>0} \subset \mathrm{L}^2(\Gamma_1)$ is bounded and, therefore, there exists a subsequence of it $\{v_{h_k}\}_{h_k>0}$ such that $\lim_{h_k\to 0}\|v_{h_k} - v\|_{\mathrm{L}^2(\Gamma_1)} = 0$. Since $J$ is weakly inferior semi-continuous in the Hilbert space $\mathrm{L}^2(\Gamma_1)$, it follows that $0 \le J(v) \le \liminf_{h_k\to 0} J(v_{h_k}) = 0$ and this yields $J(v) = 0$.

Hence the uniqueness of $v^*$ implies that $v_h$ converges weakly to $v = v^*$ in $\mathrm{L}^2(\Gamma_1)$. From the well-posedness of problems (2.4) and (2.5), see Proposition 2.5, it follows that $\lim_{h\to 0}\|u_h - u^{(\mathrm{ex})}\|_{\mathrm{L}^2(\Omega)} = 0$.

□

**FEM approximation of gradient** (3.4)**.** The FEM approximation of $J'(v)$, $v \in \mathrm{H}^{1/2}(\Gamma_1)$, is defined as

$$J_h'(v) := -\mathscr{N}_{\boldsymbol{\nu}}^*\left(\psi_h^{(1)} + \psi_h^{(2)}\right) \in \mathrm{H}^{1/2}(\Gamma_1), \quad \forall\, v \in \mathrm{H}^{1/2}(\Gamma_1), \tag{5.5}$$

where $\psi_h^{(1)}$ and $\psi_h^{(2)}$ are the unique FEM solutions to adjoint problems (3.5) and (3.6), respectively, whilst $u_h^{(1)}(v)$ and $u_h^{(2)}(v)$ are the unique FEM solutions to direct problems (2.4) and (2.5), respectively.

**Theorem 5.2** (Convergence of the FEM approximation of gradient (3.4))**.** *Let* $J'(v)$, $v \in \mathrm{H}^{1/2}(\Gamma_1)$*, be defined according to* (3.23) *and* $J_h'(v)$, $v \in \mathrm{H}^{1/2}(\Gamma_1)$*, be its FEM approximation given by* (5.5)*. Then*

$$\lim_{h\to 0}\left\|J_h'(v) - J'(v)\right\|_{\mathrm{H}^{1/2}(\Gamma_1)} = 0\,.$$

*Proof.* The high-order regularity result given by Remark 2.2 and the convergent FEM approximation used for solving the adjoint problems (3.5) and (3.6) [18] imply that $\lim_{h\to 0}\|\psi_h^{(\ell)} - \psi^{(\ell)}\|_{\mathrm{H}^2(\Omega)} = 0$, $\ell = 1,2$. Therefore, using the FEM approximation of the Neumann condition on $\Gamma_{1,h}$ yields

$$\lim_{h\to 0}\left\|\mathscr{N}_{\boldsymbol{\nu}}^*\psi_h^{(\ell)}|_{\Gamma_1} - \mathscr{N}_{\boldsymbol{\nu}}^*\psi^{(\ell)}|_{\Gamma_1}\right\|_{\mathrm{H}^{1/2}(\Gamma_1)} = 0\,, \quad \ell = 1,2. \tag{5.6}$$

Clearly, relation (5.6) implies that

$$\lim_{h\to 0} \left\| \mathscr{N}_{\boldsymbol{\nu}}^{*}\big(\psi_h^{(1)} + \psi_h^{(2)}\big)|_{\Gamma_1} - \mathscr{N}_{\boldsymbol{\nu}}^{*}\big(\psi^{(1)} + \psi^{(2)}\big)|_{\Gamma_1} \right\|_{\mathrm{H}^{1/2}(\Gamma_1)} = 0$$

and this concludes the proof. □

## 6. Numerical results

In this section, we present the performance of the wGDM introduced in Section 3.3 for the Cauchy problem (2.1) and (2.3) in a two-dimensional ($d = 2$) doubly connected domain with a smooth boundary. More precisely, we consider the annular domain $\Omega := \big\{\mathbf{x} = (x_1, x_2) \in \mathbb{R}^2 \;\big|\; r_{\mathrm{int}} < \rho(\mathbf{x}) < r_{\mathrm{out}},\ \theta(\mathbf{x}) \in [0, 2\pi)\big\}$, where $r_{\mathrm{int}} = 0.5$ and $r_{\mathrm{out}} = 1.0$, with the boundary $\partial\Omega = \Gamma_0 \cup \Gamma_1$ such that $\Gamma_0 = \Gamma_{\mathrm{out}} = \{\mathbf{x} \in \mathbb{R}^2 \;|\; \rho(\mathbf{x}) = r_{\mathrm{out}},\ \theta(\mathbf{x}) \in [0, 2\pi)\}$ and $\Gamma_1 = \Gamma_{\mathrm{int}} = \{\mathbf{x} \in \mathbb{R}^2 \;|\; \rho(\mathbf{x}) = r_{\mathrm{int}},\ \theta(\mathbf{x}) \in [0, 2\pi)\}$. We further assume that the solid occupying $\Omega$ is characterised by the homogeneous thermal conductivity tensor $\mathbf{K} = \big(k_{ij}\big)_{i,j=1,2} \in \mathbb{R}^{2\times 2}$, where $k_{11} = 1.0$, $k_{12} = k_{21} = 0.2$ and $k_{22} = 0.4$, in case of Examples 6.1 and 6.2, whilst for Example 6.3 the thermal conductivity tensor is considered to be non-smooth, satisfies Assumptions (A1) and (A2), and is given by

$$\mathbf{K} = \begin{cases} \begin{bmatrix} 5.0 & 1.0 \\ 1.0 & 2.0 \end{bmatrix} & \text{if } \ r_{\mathrm{int}} \le \rho(\mathbf{x}) \le \big(r_{\mathrm{int}} + r_{\mathrm{out}}\big)/2 \\ \begin{bmatrix} 1.0 & 0.4 \\ 0.4 & 0.2 \end{bmatrix} & \text{if } \ \big(r_{\mathrm{int}} + r_{\mathrm{out}}\big)/2 < \rho(\mathbf{x}) \le r_{\mathrm{out}}. \end{cases} \tag{6.1}$$

**Example 6.1.** Assume that $u^{(\mathrm{ex})} \in \mathrm{H}^1(\Omega)$ is the unique solution, obtained by the FEM with $n_{\mathrm{FEM}} = 43680$ nodes, to the Dirichlet problem for the Laplace–Beltrami equation (2.1) with the regular data on $\Gamma_0$, $u^{(\mathrm{ex})}\big|_{\Gamma_0} \in \mathrm{H}^{1/2}(\Gamma_0)$, given by

$$u^{(\mathrm{ex})}(x_1, x_2) = \cos x_1 \cosh x_2 + \sin x_1 \sinh x_2\,, \quad (x_1, x_2) \in \Gamma_0\,, \tag{6.2}$$

and the irregular data on $\Gamma_1$, $u^{(\mathrm{ex})}\big|_{\Gamma_1} = v_h\big|_{\Gamma_1}$, where $v_h \in \mathrm{H}^{1/2}(\Gamma_1)$ is the $\mathrm{L}^2-$projection (5.1) of the step function $v \in \mathrm{L}^2(\Gamma_1) \setminus \mathrm{H}^{1/2}(\Gamma_1)$ defined by

$$v(x_1, x_2) = \begin{cases} -1\,, (x_1, x_2) \in \Gamma_1 \cap \big\{(x_1, x_2) \in \mathbb{R}^2 \;|\; x_2 < 0\big\} \\ \ \ 1\,, (x_1, x_2) \in \Gamma_1 \cap \big\{(x_1, x_2) \in \mathbb{R}^2 \;|\; x_2 > 0\big\}. \end{cases}$$

Note that $q^{(\mathrm{ex})}\big|_{\partial\Omega}$ is defined by (2.2) with $u\big|_{\partial\Omega} = u^{(\mathrm{ex})}\big|_{\partial\Omega}$ given above, whilst $q^{(\mathrm{ex})}\big|_{\Gamma_1} \notin \mathrm{H}^{-1/2}(\Gamma_1)$.

**Example 6.2.** Let $u^{(\mathrm{ex})} \in \mathrm{H}^1(\Omega)$ be the unique solution, retrieved analogously to that corresponding to Example 6.1, for the Dirichlet problem associated with Laplace–Beltrami's equation (2.1) with the regular data on $\Gamma_0$ given by (6.2) and $u^{(\mathrm{ex})}\big|_{\Gamma_1} = v\big|_{\Gamma_1}$, where

$$v(x_1, x_2) = \sqrt{\operatorname{atan}\big(x_2/x_1\big)}\,, \quad (x_1, x_2) \in \Gamma_1\,.$$

Yet again, $q^{(\mathrm{ex})}\big|_{\partial\Omega}$ is given by relation (2.2) with $u\big|_{\partial\Omega} = u^{(\mathrm{ex})}\big|_{\partial\Omega}$, whereas $q^{(\mathrm{ex})}\big|_{\Gamma_1} \notin \mathrm{L}^2(\Gamma_1)$.

**Example 6.3.** We let $u^{(\mathrm{ex})} \in \mathrm{H}^1(\Omega)$ be the unique solution, obtained *via* the FEM for the anisotropic Laplace equation (2.1) with the same regular Dirichlet data on $\Gamma_0$ and irregular Dirichlet data on $\Gamma_1$ as those corresponding to Example 6.1 and $\mathbf{K}$ given by (6.1), whilst $q^{(\mathrm{ex})}\big|_{\partial\Omega}$ is defined by (2.2) with $u\big|_{\partial\Omega} = u^{(\mathrm{ex})}\big|_{\partial\Omega}$.

All of the direct problems for the Laplace-Beltrami equation considered herein have been solved numerically by the conforming FEM described in Section 5 with various numbers of nodes, namely $n_{\mathrm{FEM}} \in \{756, 2856, 11088\}$. We note that the FEM discretisations have been chosen carefully in order to avoid the so-called inverse crime.

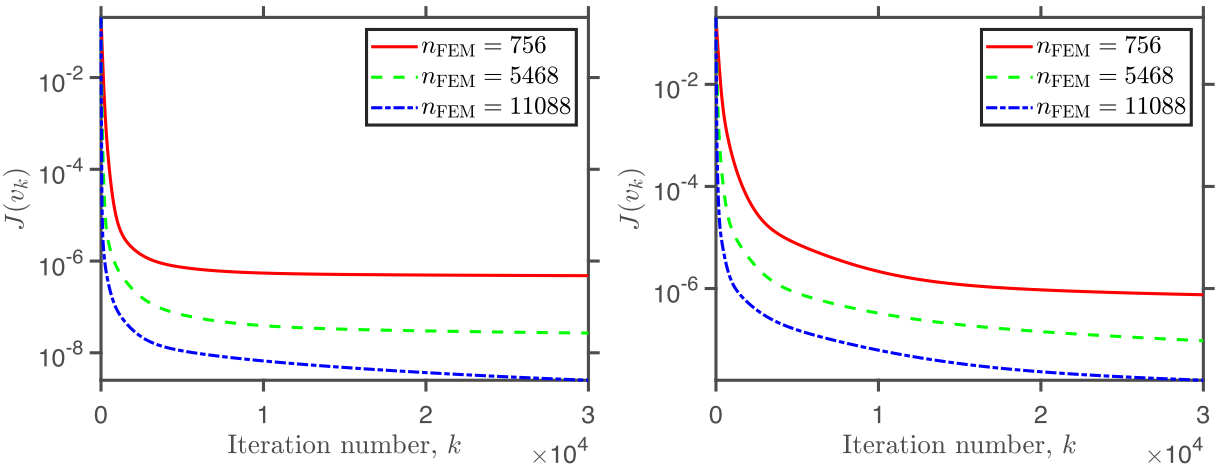


FIGURE 2. Evolution of functional $J$ with respect to the number of iterations $k$, retrieved by (a) the wGDM with $\gamma = 10^{-4}$, and (b) the GDM with $\gamma = 10^{-3}$, respectively, $n_{\text{FEM}} \in \{756, 2856, 11088\}$ and exact Cauchy data on $\Gamma_0$, for Example 6.2.

### 6.1. Results with exact data

Next, we set the initial guess for $u\big|_{\Gamma_1}$ as

$$v_0(\mathbf{x}) = 0, \quad \mathbf{x} \in \Gamma_1,$$

and investigate the accuracy and convergence of the numerically reconstructed temperatures and normal heat fluxes on the under-specified boundary $\Gamma_1$, as well as the features of the functional used in the minimisation process, for exact Cauchy data $u\big|_{\Gamma_0} = u^{(\text{ex})}\big|_{\Gamma_0}$ and $q\big|_{\Gamma_0} = q^{(\text{ex})}\big|_{\Gamma_0}$.

**Convergence of functional $J$.** The evolution of functional $J$ given by (3.2) as a function of the number of iterations, $k$, obtained using the wGDM with $\gamma = 10^{-4}$ and the GDM with $\gamma = 10^{-3}$, and various FEM discretisations, *i.e.* $n_{\text{FEM}} \in \{756, 2856, 11088\}$, for Example 6.2, is presented in Figures 2a and 2b, respectively. It can be seen that, for both algorithms and all of the FEM meshes considered, the corresponding functional decreases rapidly until a certain iteration number, after which it reaches a plateau region approximating zero, *i.e.* $J$ is convergent with respect to increasing the number of iterations. The main features of the wGDM and GDM can be noticed in Figure 2, namely the minimisation of functional $J$ in the corresponding function space is very rapid and, at the same time, very good, whilst the regularizing effect of $J$ occurs when it reaches the plateau region. Moreover, in case of both the wGDM and the GDM, for a fixed number of iterations, the values of the corresponding functional (3.2) decrease as $n_{\text{FEM}}$ increases, thus showing the convergence of both these algorithms with respect to refining the FEM mesh. By comparing Figures 2a and 2b, it can be seen that, for each FEM triangulation used and each iteration number, the values of $J$ obtained using the wGDM are lower than those retrieved with the GDM and this emphasises the main advantage of the wGDM, namely its suitability for the approximation of merely $\text{L}^2-$boundary data.

**Accuracy errors.** To assess the accuracy of the wGDM, we define the following accuracy errors for the numerically reconstructed boundary temperature and normal heat flux in the $\text{L}^2(\Gamma_1)$ norm, as well as with

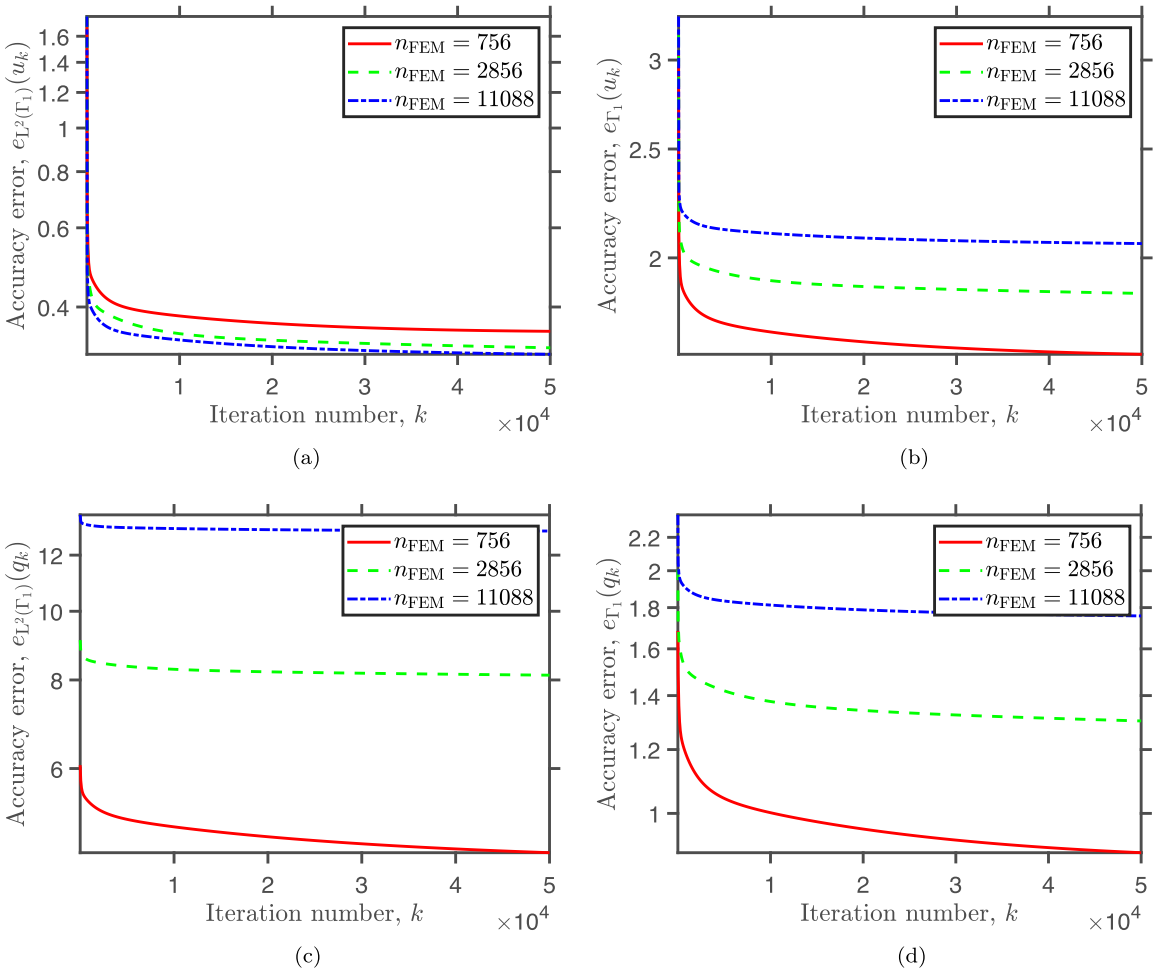


FIGURE 3. The accuracy errors (a) $e_{\mathrm{L}^2(\Gamma_1)}(u_k)$, (b) $e_{\Gamma_1}(u_k)$, (c) $e_{\mathrm{L}^2(\Gamma_1)}(q_k)$, and (d) $e_{\Gamma_1}(q_k)$, as functions of the number of iterations $k$, retrieved with the wGDM, $\gamma = 10^{-3}$, $n_{\mathrm{FEM}} \in \{756, 2856, 11088\}$ and exact Cauchy data on $\Gamma_0$, for Example 6.1.

respect to the norms equivalent to $\|\cdot\|_{\mathrm{H}^{1/2}(\Gamma_1)}$ and $\|\cdot\|_{\mathrm{H}^{-1/2}(\Gamma_1)}$, namely

$$e_{\mathrm{L}^2(\Gamma_1)}(u_k) := \left\|u_h^{(\mathrm{ex})} - u^{(2)}(v_k)\right\|_{\mathrm{L}^2(\Gamma_1)}, \tag{6.3a}$$

$$e_{\Gamma_1}(u_k) := \left\|u_h^{(\mathrm{ex})} - u^{(2)}(v_k)\right\|_{\Gamma_1}, \tag{6.3b}$$

$$e_{\mathrm{L}^2(\Gamma_1)}(q_k) := \left\|q_h^{(\mathrm{ex})} - q^{(2)}(v_k)\right\|_{\mathrm{L}^2(\Gamma_1)}, \tag{6.3c}$$

$$e_{\Gamma_1}(q_k) := \left\|q_h^{(\mathrm{ex})} - q^{(2)}(v_k)\right\|_{\Gamma_1}. \tag{6.3d}$$

Here $u_h^{(\mathrm{ex})}$ and $q_h^{(\mathrm{ex})}$ are the FEM functions associated with $u^{(\mathrm{ex})}$ and $q^{(\mathrm{ex})}$, respectively, whilst $u^{(2)}(v_k)$ and $q^{(2)}(v_k)$ are the corresponding numerical temperature and normal heat flux, respectively, retrieved after $k$ iterations by solving problem (3.24b) *via* the FEM. The error in predicting the temperature at internal points may also be evaluated using the corresponding $\mathrm{L}^2-$ or $\mathrm{H}^1-$norm. Nonetheless, this is not pursued here since

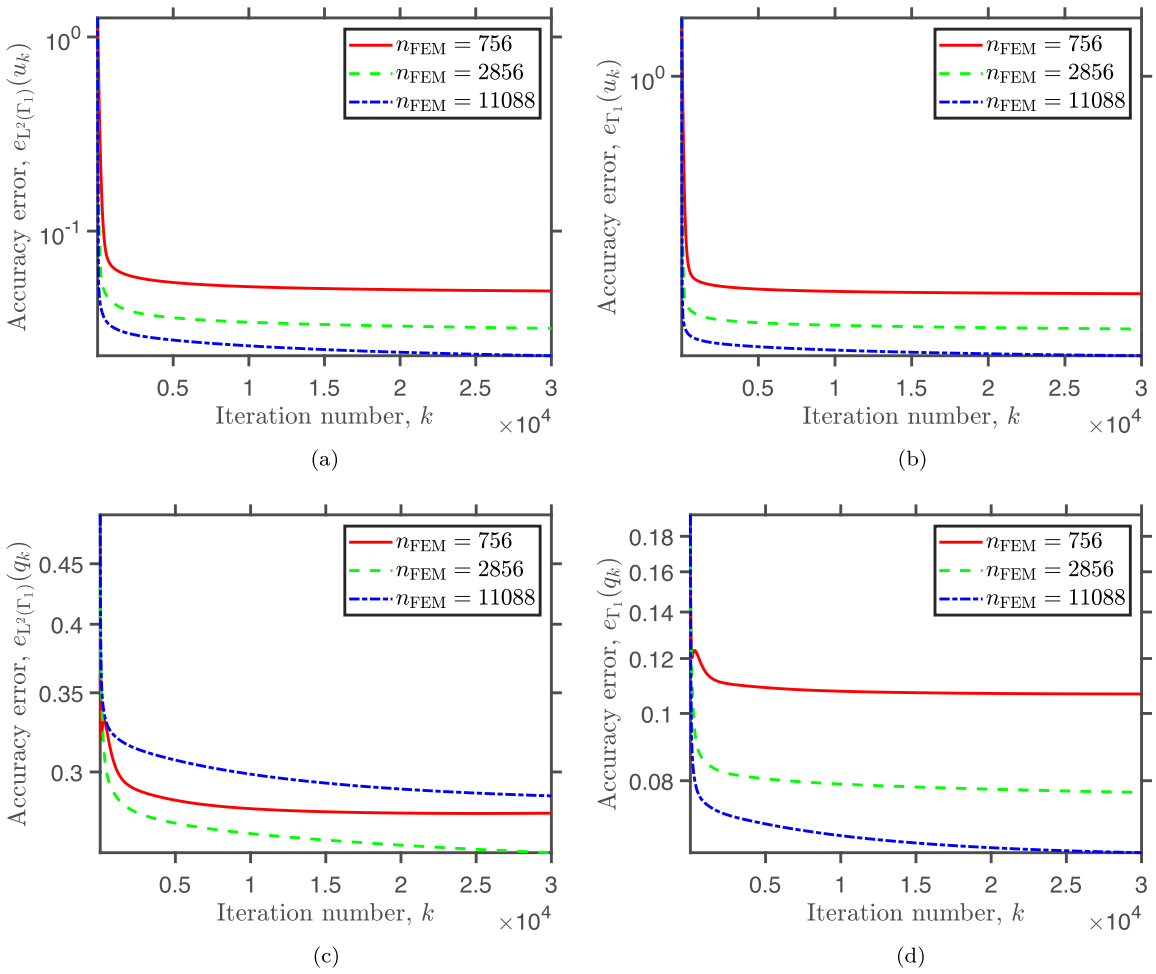


FIGURE 4. The accuracy errors (a) $e_{L^2(\Gamma_1)}(u_k)$, (b) $e_{\Gamma_1}(u_k)$, (c) $e_{L^2(\Gamma_1)}(q_k)$, and (d) $e_{\Gamma_1}(q_k)$, as functions of the number of iterations $k$, retrieved by the wGDM, $\gamma = 10^{-4}$, $n_{FEM} \in \{756, 2856, 11088\}$ and exact Cauchy data on $\Gamma_0$, for Example 6.2.

this error has an evolution with respect to the number of iterations performed similar to that of the errors given by relations (6.3a)–(6.3d).

The accuracy errors $e_{L^2(\Gamma_1)}(u_k)$, $e_{\Gamma_1}(u_k)$, $e_{L^2(\Gamma_1)}(q_k)$ and $e_{\Gamma_1}(q_k)$ as functions of the number of iterations $k$, with $\gamma = 10^{-3}$ and $n_{FEM} \in \{756, 2856, 11088\}$, for Example 6.1, are presented in Figures 3a–3d, respectively, on a semi-logarithmic scale. From these figures it can be seen that, for each FEM discretisation considered, $e_{L^2(\Gamma_1)}(u_k)$, $e_{\Gamma_1}(u_k)$, $e_{L^2(\Gamma_1)}(q_k)$ and $e_{\Gamma_1}(q_k)$ decrease as $k$ increases, *i.e.* the wGDM is convergent with respect to increasing $k$. We also remark that the accuracy errors (6.3a)–(6.3d) decrease until a specific iteration number and they reach a plateau region becoming stable after that iteration. At each iteration $k$, the values of $e_{L^2(\Gamma_1)}(u_k)$ decrease with respect to increasing $n_{FEM}$, *i.e.* the wGDM produces a sequence of approximations convergent to the exact solution of the Cauchy problem (2.1) and (2.3) as $h \searrow 0$. However, as expected, the accuracy errors $e_{\Gamma_1}(u_k)$, $e_{L^2(\Gamma_1)}(q_k)$ and $e_{\Gamma_1}(q_k)$ increase with respect to refining the FEM mesh since the Dirichlet data on $\Gamma_1$ is a jump function, *i.e.* $u^{(ex)}|_{\Gamma_1} \in L^2(\Gamma_1) \setminus H^{1/2}(\Gamma_1)$ and $q^{(ex)}|_{\Gamma_1} \notin H^{-1/2}(\Gamma_1)$.

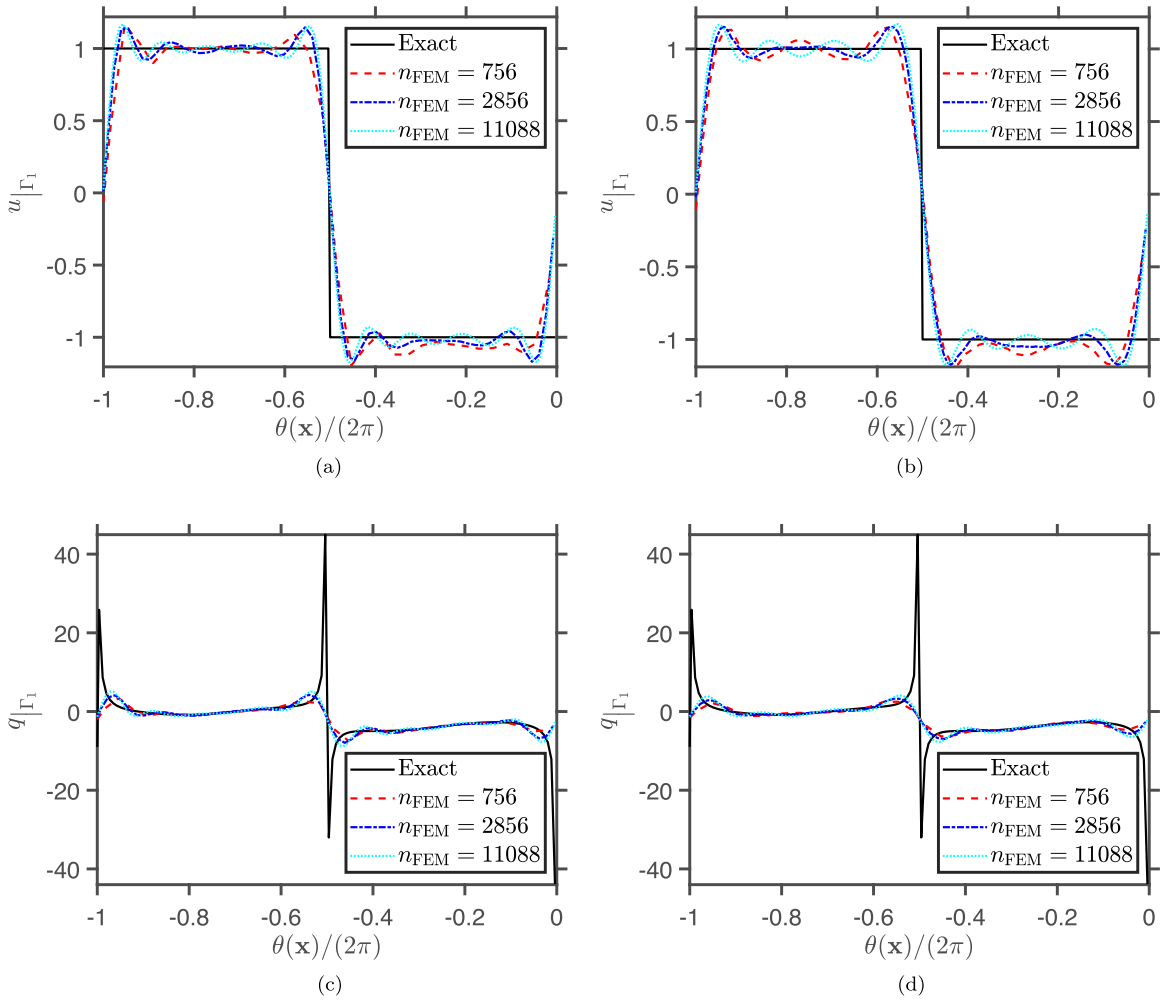


FIGURE 5. The analytical and numerical (a) and (b) temperatures, and (c) and (d) normal heat fluxes on $\Gamma_1 = \Gamma_{\mathrm{int}}$, obtained using the wGDM with $\gamma = 10^{-4}$, the GDM with $\gamma = 10^{-3}$, $k = 50000$ iterations, $n_{\mathrm{FEM}} \in \{756, 2856, 11088\}$ and exact Cauchy data on $\Gamma_0$, for Example 6.1.

Figures 4a–4d present, on a semi-logarithmic scale, the evolution of the accuracy errors (6.3a)–(6.3d), respectively, with respect the number of iterations $k$, retrieved with the wGDM, $\gamma = 10^{-4}$ and $n_{\mathrm{FEM}} \in \{756, 2856, 11088\}$, for Example 6.2. It can be seen from these figures that, for each fixed value of $n_{\mathrm{FEM}}$, $e_{\mathrm{L}^2(\Gamma_1)}(u_k)$, $e_{\Gamma_1}(u_k)$, $e_{\mathrm{L}^2(\Gamma_1)}(q_k)$ and $e_{\Gamma_1}(q_k)$ decrease as $k$ increases, *i.e.* the wGDM is convergent with respect to increasing the number of iterations. It can also be noticed from Figures 4a–4d that all of the accuracy errors given by (6.3a)–(6.3d) decrease until a specific iteration number, after which they become stable, *i.e.* a plateau region is attained by these errors. Moreover, at each iteration $k$, the values of $e_{\mathrm{L}^2(\Gamma_1)}(u_k)$, $e_{\Gamma_1}(u_k)$ and $e_{\Gamma_1}(q_k)$ decrease as $n_{\mathrm{FEM}}$ increases, *i.e.* the wGDM is convergent with respect to decreasing the FEM mesh size. As expected, $e_{\mathrm{L}^2(\Gamma_1)}(q_k)$ increases as $h \searrow 0$ since $q^{(\mathrm{ex})}|_{\Gamma_1} \notin \mathrm{L}^2(\Gamma_1)$.

**Convergence of the numerical reconstructions.** Figures 5a and 5c display the exact and numerical temperatures and normal heat fluxes on $\Gamma_1$, retrieved by the wGDM with $\gamma = 10^{-3}$, $n_{\mathrm{FEM}} \in \{756, 2856, 11088\}$ and

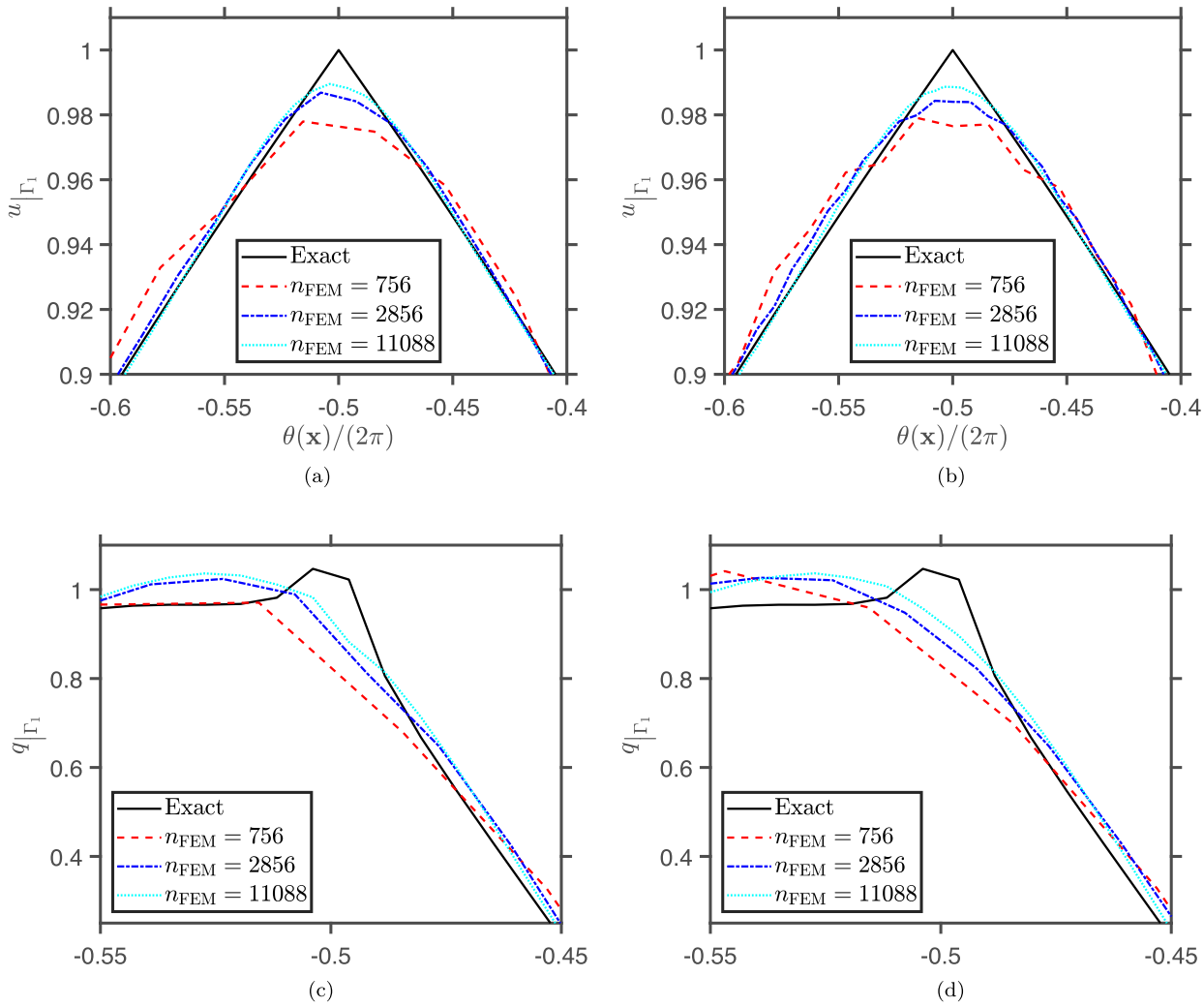


FIGURE 6. The analytical and numerical (a) and (b) temperatures, and (c) and (d) normal heat fluxes on $\Gamma_1 = \Gamma_{\text{int}}$, obtained using the wGDM with $\gamma = 10^{-4}$, the GDM with $\gamma = 10^{-3}$, $k = 30,000$ iterations, $n_{\text{FEM}} \in \{756, 2856, 11088\}$ and exact Cauchy data on $\Gamma_0$, Example 6.2.

exact Cauchy data on $\Gamma_0$, for Example 6.1, whilst similar results are presented in Figures 5b and 5d, however, obtained using the GDM with $\gamma = 10^{-3}$. It can be seen from these figures that, for both the wGDM and the GDM, the numerically reconstructed temperatures and normal heat fluxes on $\Gamma_1$, for exact Cauchy data on $\Gamma_0$, converge towards their exact counterparts as $n_{\text{FEM}}$ increases, *i.e.* yet again, both algorithms converge with respect to refining the FEM mesh. By comparing Figures 5a and 5c, and Figures 5b and 5d, it can be seen that the wGDM provides very good approximations for non-smooth Dirichlet and Neumann data on $\Gamma_1$, whereas the GDM also produces good reconstructions for the missing temperature and normal heat flux on $\Gamma_1$, however, as expected, much smoother than the previous ones.

Figures 6a–6d illustrate the exact and numerical results for the temperature and the normal heat flux on $\Gamma_1$, obtained using the wGDM with $\gamma = 10^{-4}$ and the GDM with $\gamma = 10^{-3}$, respectively, and $n_{\text{FEM}} \in \{756, 2856, 11,088\}$, for Example 6.2. By comparing Figures 5 and 6, it can be seen that the numerical results

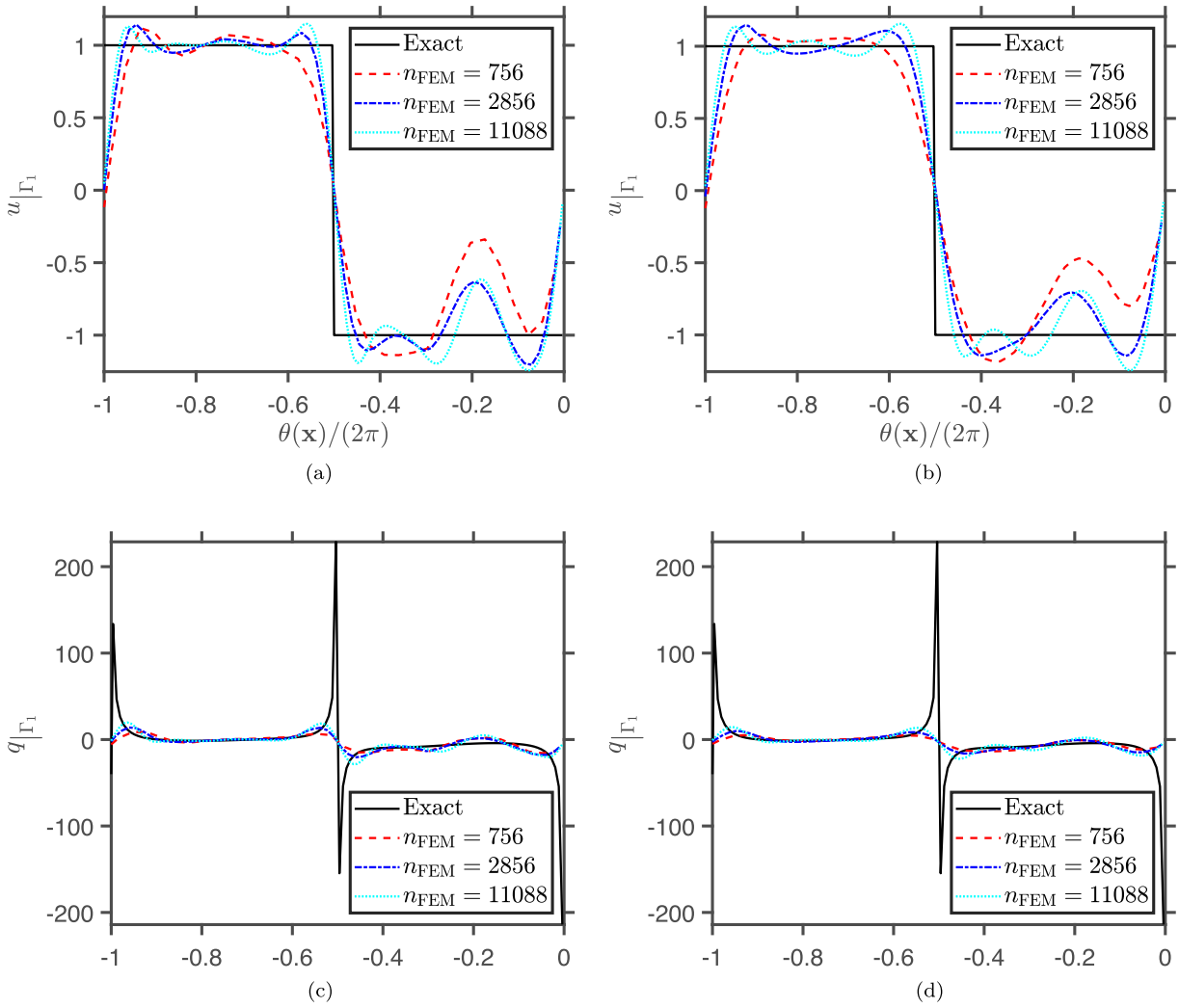


FIGURE 7. The analytical and numerical (a) and (b) temperatures, and (c) and (d) normal heat fluxes on $\Gamma_1 = \Gamma_{\text{int}}$, obtained using the wGDM with $\gamma = 10^{-4}$, the GDM with $\gamma = 10^{-3}$, $k = 1000$ iterations, $n_{\text{FEM}} \in \{756, 2856, 11088\}$ and exact Cauchy data on $\Gamma_0$, for Example 6.3.

retrieved for Example 6.2 behave analogously to their counterparts obtained for Example 6.1, hence emphasising, yet again, the advantage of the wGDM over the GDM when reconstructing non-smooth boundary data.

Figures 7a and 7c, and 7b and 7d present the exact and numerical temperatures and normal heat fluxes on $\Gamma_1$, obtained by the wGDM with $\gamma = 10^{-4}$ and the GDM with $\gamma = 10^{-3}$, respectively, and $n_{\text{FEM}} \in \{756, 2856, 11088\}$, for Example 6.3. A comparison of Figures 5 and 7 shows that the numerical results retrieved for Example 6.3 preserve the same features as those corresponding to Example 6.1. However, higher oscillations occur in the numerical reconstructions associated with the former example and these are caused by the non-smooth character of the thermal conductivity tensor given by (6.1).

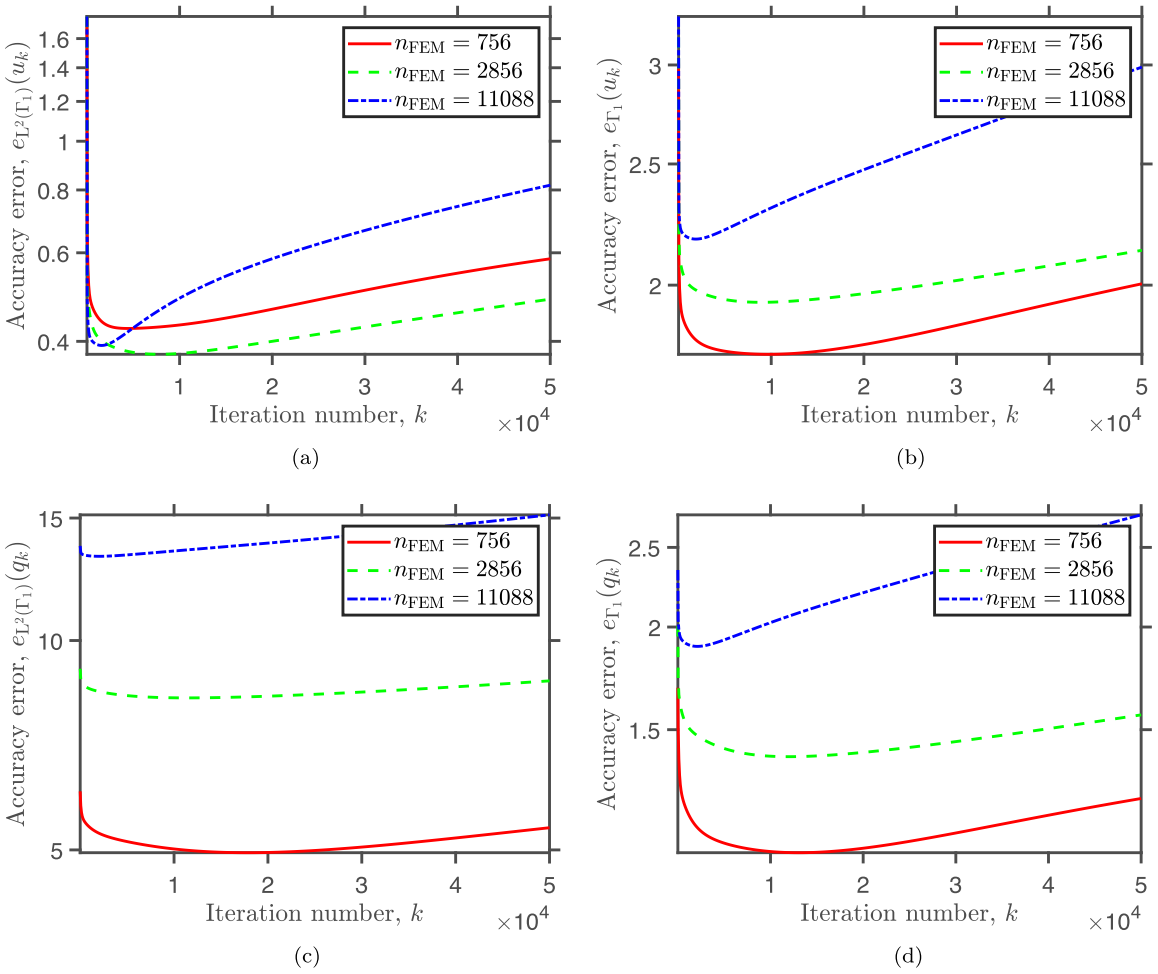


FIGURE 8. The accuracy errors (a) $e_{L^2(\Gamma_1)}(u_k)$, (b) $e_{\Gamma_1}(u_k)$, (c) $e_{L^2(\Gamma_1)}(q_k)$, and (d) $e_{\Gamma_1}(q_k)$, as functions of the number of iterations $k$, retrieved with the wGDM, $\gamma = 10^{-3}$, $n_{FEM} \in \{756, 2856, 11088\}$ and $p_u = p_q = 5\%$, for Example 6.1.

### 6.2. Results with noisy data

The inherent errors in the data on $\Gamma_0$ are simulated by perturbing the corresponding exact values as

$$u_\delta^*(\mathbf{x}) = u^{(ex)}(\mathbf{x})\,(1 + p_u\,\delta)\,, \quad \mathbf{x} \in \Gamma_0\,,$$
$$q_\delta^*(\mathbf{x}) = q^{(ex)}(\mathbf{x})\,(1 + p_q\,\delta)\,, \quad \mathbf{x} \in \Gamma_0\,,$$

where $p_u$ and $p_q$ are the percentages of noise added to the Dirichlet and Neumann data on $\Gamma_0$, respectively, and $\delta = -1 + 2\,\texttt{rand}(\cdot)$ is a pseudorandom uniform number from $[-1, 1]$ generated by the MATLAB® command `rand`$(\cdot)$. In addition, we assume that estimates on the amount of noise added to the temperature data on $\Gamma_0$ are available in the $L^2-$norm and in that equivalent to the $H^{1/2}-$norm, namely

$$\epsilon_{L^2(\Gamma_0)} \coloneqq \|u_\delta^* - u^*\|_{L^2(\Gamma_0)}\,, \tag{6.4a}$$
$$\epsilon_{\Gamma_0} \coloneqq \|u_\delta^* - u^*\|_{\Gamma_0}\,. \tag{6.4b}$$

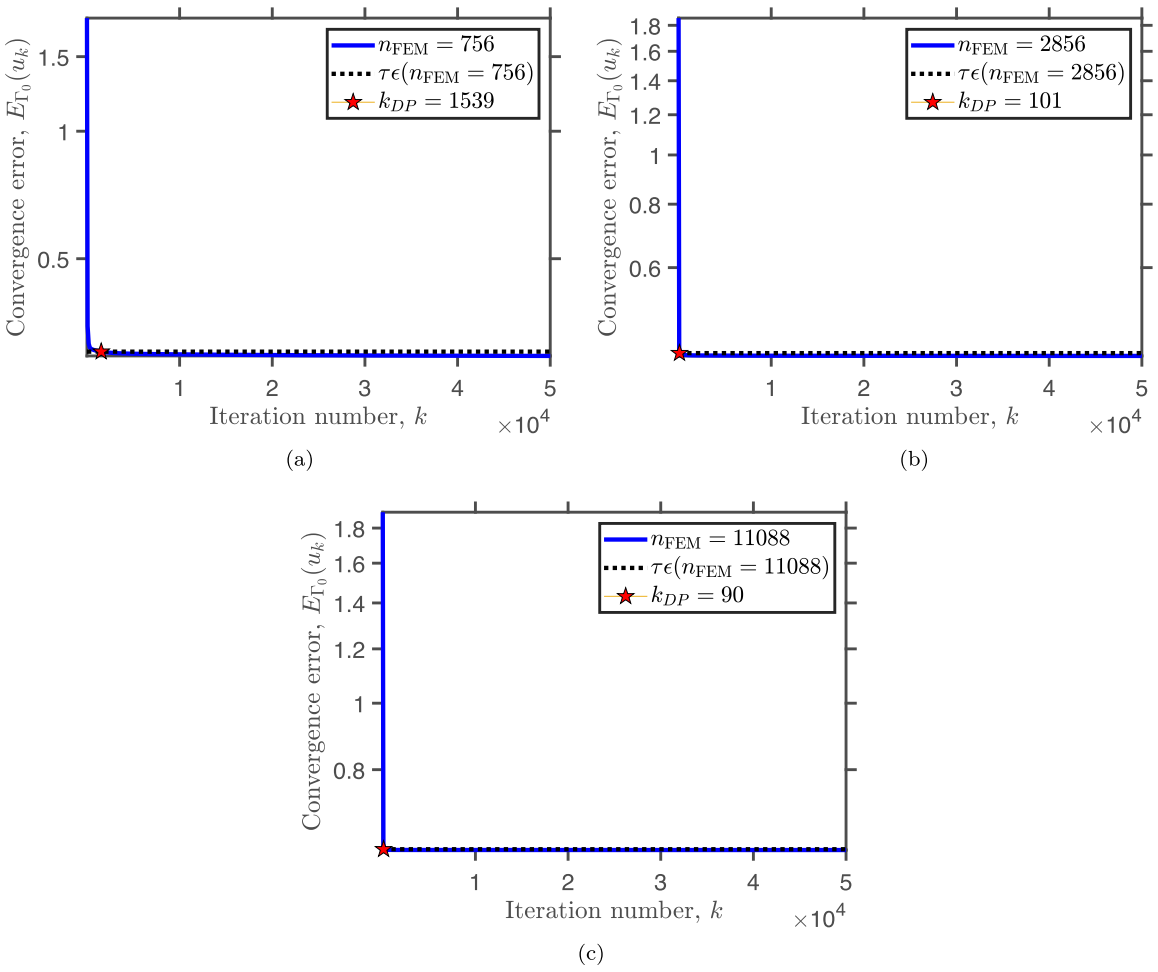


FIGURE 9. The convergence error $E_{\Gamma_0}(u_k)$, as a function of the number of iterations $k$, and the corresponding values for $\tau\epsilon_{\Gamma_0}$, obtained using the wGDM, $\gamma = 10^{-3}$, $p_u = p_q = 5\%$, and (a) $n_{\text{FEM}} = 756$, (b) $n_{\text{FEM}} = 2856$, and (c) $n_{\text{FEM}} = 11088$, for Example 6.1.

Figures 8a–8d display the accuracy errors defined by relations (6.3a)–(6.3d), respectively, as functions of $k$, obtained with $n_{\text{FEM}} \in \{756, 2856, 11088\}$ and $p_u = p_q = 5\%$, for Example 6.1. It can be observed that, for each FEM triangulation, these errors decrease abruptly until a certain iteration number, after which they start to increase since the effect of noise added to the data on $\Gamma_0$ becomes dominant in the reconstructions of both the temperature and the normal heat flux on $\Gamma_1$. More specifically, by continuing the iterative procedure beyond that specific number of iterations, the numerical Dirichlet and Neumann conditions on $\Gamma_1$ become highly oscillatory and unbounded, *i.e.* the Cauchy problem (2.1) and (2.3) is highly unstable. Therefore, a regularizing/stabilising stopping criterion is required for perturbed Cauchy data in order to stop the wGDM around the iteration number at which the minimum in the accuracy errors is attained.

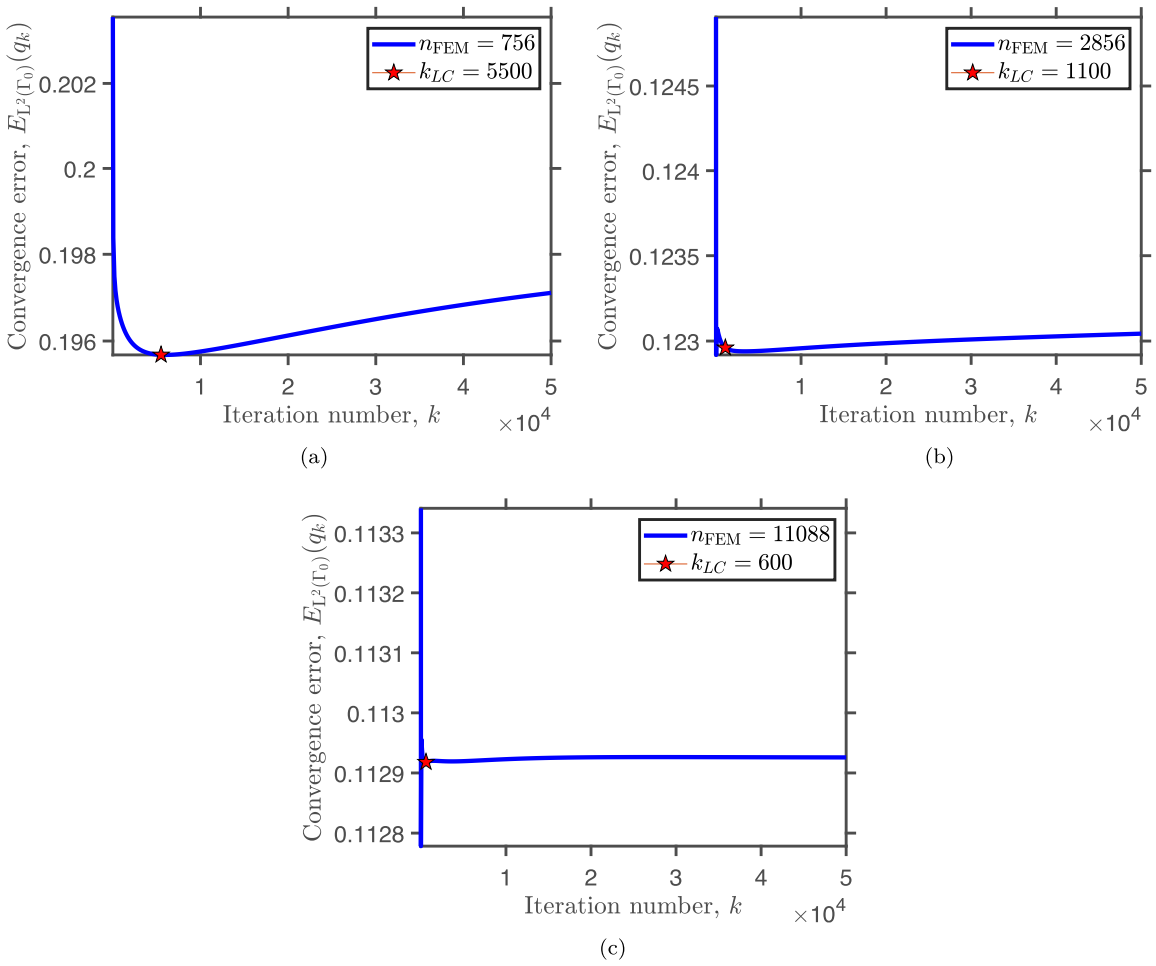


FIGURE 10. The convergence error $E_{\text{L}^2(\Gamma_0)}(q_k)$, as a function of the number of iterations $k$, and $k_{\text{LC}}$ given by the L-curve criterion, obtained using the wGDM, $\gamma = 10^{-3}$, $p_u = p_q = 5\%$, and (a) $n_{\text{FEM}} = 756$, (b) $n_{\text{FEM}} = 2856$, and (c) $n_{\text{FEM}} = 11088$, for Example 6.1.

**Regularizing stopping criteria.** The errors in the Dirichlet data on the over-prescribed boundary $\Gamma_0$, with respect to the $\text{L}^2-$norm and that equivalent to the $\text{H}^{1/2}-$norm, are defined by

$$E_{\text{L}^2(\Gamma_0)}(u_k) := \left\| u_\delta^* - u^{(2)}(v_k) \right\|_{\text{L}^2(\Gamma_0)}, \tag{6.5a}$$

$$E_{\Gamma_0}(u_k) := \left\| u_\delta^* - u^{(2)}(v_k) \right\|_{\Gamma_0}. \tag{6.5b}$$

According to the discrepancy principle of Morozov [39], for perturbed Cauchy data, the iterative process associated with the wGDM is stopped at the iteration number given by

$$k_{\text{DP}} := \min\left\{ k \in \mathbb{Z}_+ \;\middle|\; E(u_k) < \tau\epsilon \right\}, \tag{6.6}$$

where $E(u_k)$ is the corresponding error given by either (6.5a) or (6.5b), $\epsilon$ is the amount of noise added to $u^{(\text{ex})}|_{\Gamma_0}$ given by either (6.4a) or (6.4b), and $\tau > 1$ is a constant to be prescribed [24].

Figures 9a–9c illustrate the evolution of the convergence error $E_{\Gamma_0}(u_k)$ as a function of the number of iterations and the corresponding values for $\tau\epsilon_{\Gamma_0}$, obtained with the wGDM, $\gamma = 10^{-3}$, $n_{\text{FEM}} \in \{756, 2856, 11088\}$ and

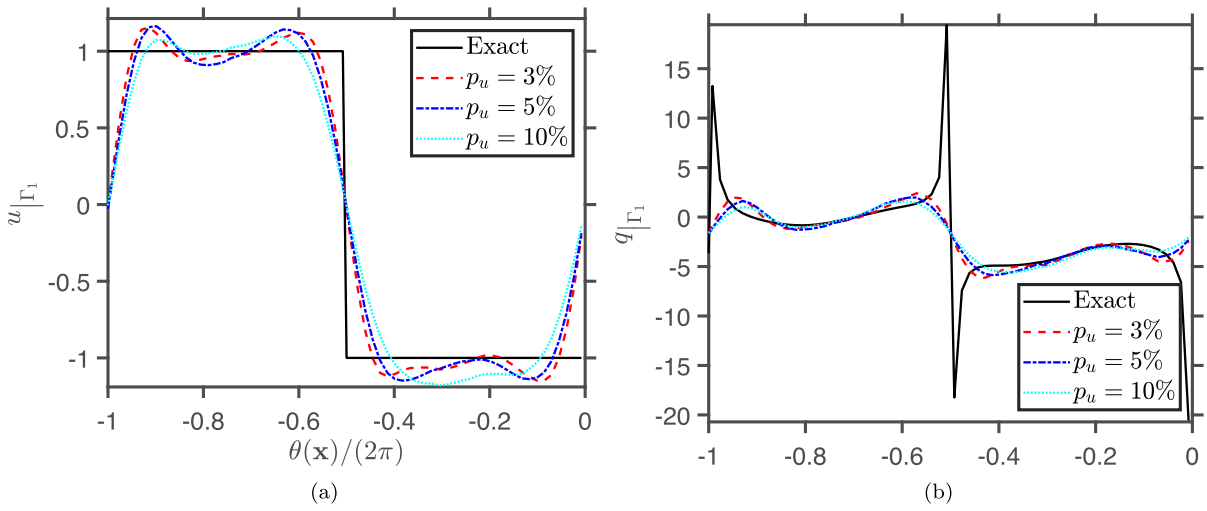


FIGURE 11. The analytical and numerical (a) temperatures, and (b) normal heat fluxes on $\Gamma_1 = \Gamma_{\text{int}}$, retrieved by the wGDM, $\gamma = 10^{-4}$, $k = k_{\text{DP}}$, $n_{\text{FEM}} = 2856$ and $p_u = p_q \in \{3\%, 5\%, 10\%\}$, for Example 6.1.

$p_u = p_q = 5\%$, for Example 6.1. One can remark from these figures that for all FEM meshes used, $E_{\Gamma_0}(u_k)$ decreases very abruptly until a certain iteration number, after which it reaches a plateau. By comparing Figures 8 and 9, it may be concluded that Morozov's discrepancy principle (6.6) for the error given by (6.5b) is very efficient in locating the iteration number where $e_{\mathrm{L}^2(\Gamma_1)}(u_k)$, $e_{\mathrm{L}^2(\Gamma_1)}(q_k)$, $e_{\Gamma_1}(u_k)$ and $e_{\Gamma_1}(q_k)$ attain their corresponding minimum and the wGDM should be terminated. It is worth mentioning that similar results have been obtained for the stopping criterion (6.6) in conjunction with the convergence error $E_{\mathrm{L}^2(\Gamma_0)}(u_k)$, however the corresponding results have not been presented.

We also consider the convergence error for the normal heat flux on $\Gamma_0$ in the $\mathrm{L}^2-$norm, *i.e.*

$$E_{\mathrm{L}^2(\Gamma_0)}(q_k) := \left\| q_\delta^* - q^{(2)}(v_k) \right\|_{\mathrm{L}^2(\Gamma_0)}. \tag{6.7}$$

An alternative stopping rule to (6.6) is the L-curve method [25] which terminates the iterative procedure at iteration $k_{\text{LC}}$ that corresponds to the maximum curvature of the discrete curve $\left\{ \left( \log_{10} k, \log_{10} E_{\mathrm{L}^2(\Gamma_0)}(q_k) \right) \mid k \geq 0 \right\}$. Figures 10a–10c illustrate the evolution of $E_{\mathrm{L}^2(\Gamma_0)}(q_k)$ as a function of $k$ and the corresponding iteration number performed according to Hansen's L-curve criterion, $k_{\text{LC}}$, using $n_{\text{FEM}} \in \{756, 2856, 11088\}$ and $p_u = p_q = 5\%$, for Example 6.1. It can be seen from these figures that for all FEM triangulations considered, the convergence error (6.7) decreases very abruptly until a certain iteration number, after which it slowly starts to increase due to the instability of the inverse Cauchy problem (2.1)–(2.3). From Figures 8 and 10 it may be concluded that the L-curve method for the convergence error (6.7) may also be used as a regularizing stopping rule for the wGDM.

**Stability of the numerical reconstruction.** In the following, we fix $n_{\text{FEM}} = 2856$ and study the numerical stability of the FEM solution obtained by the wGDM with respect to the level of noise in the Cauchy data on $\Gamma_0$. Figures 11a and 11b present the analytical and numerical solutions for the temperature and the normal heat flux on $\Gamma_1$, respectively, obtained using the stopping criterion (6.6) with (6.5b) and $p_u = p_q \in \{3\%, 5\%, 10\%\}$, for Example 6.1. From this figures it can be remarked that the numerical approximations for both $u|_{\Gamma_1}$ and $q|_{\Gamma_1}$ are stable, free of unbounded and rapid oscillations, showing thus the regularizing character of the discrepancy principle for the wGDM.

TABLE 1. Values of the accuracy error $e_{\mathrm{L}^2(\Gamma_1)}(u_k)$, the corresponding convergence error $E_{\mathrm{SC}}$, given by $E_{\Gamma_0}(u_k)$, $E_{\mathrm{L}^2(\Gamma_0)}(u_k)$ or $E_{\mathrm{L}^2(\Gamma_0)}(q_k)$, and the number of iterations performed, $k_{\mathrm{SC}}$, retrieved by the wGDM, $\gamma = 10^{-3}$, $n_{\mathrm{FEM}} = 2856$, $p_u = p_q \in \{3\%, 5\%, 10\%\}$, the discrepancy principle (DP) with (6.5a) or (6.5b), and the L-curve method (LC), for Example 6.1.

| Stopping Criterion | $p_u = p_q$ | $e_{\mathrm{L}^2(\Gamma_1)}(u_k)$ | $E_{\mathrm{SC}}$ | $k_{\mathrm{SC}}$ |
|---|---|---|---|---|
| DP & $E_{\Gamma_0}(u_k)$ | 3% | 4.35 (−1) | 2.44 (−1) | 420 |
| | 5% | 4.88 (−1) | 4.07 (−1) | 101 |
| | 10% | 5.47 (−1) | 8.14 (−1) | 39 |
| DP & $E_{\mathrm{L}^2(\Gamma_0)}(u_k)$ | 3% | 4.14 (−1) | 4.61 (−2) | 743 |
| | 5% | 4.51 (−1) | 7.68 (−2) | 316 |
| | 10% | 5.11 (−1) | 1.54 (−1) | 73 |
| LC & $E_{\mathrm{L}^2(\Gamma_0)}(q_k)$ | 3% | 3.98 (−1) | 9.29 (−2) | 1400 |
| | 5% | 4.10 (−1) | 1.23 (−1) | 1100 |
| | 10% | 4.42 (−1) | 2.11 (−1) | 900 |

For the sake of completeness, in Tables 1 and 2 we present the values of the accuracy error $e_{\mathrm{L}^2(\Gamma_1)}(u_k)$, the convergence error corresponding to the stopping rule employed, the number of iterations as given by the discrepancy principle (6.6), $k_{\mathrm{DP}}$, or the L-curve method, $k_{\mathrm{LC}}$, using the wGDM, $\gamma = 10^{-3}$, $n_{\mathrm{FEM}} = 2856$ and $p_u = p_q \in \{3\%, 5\%, 10\%\}$, for Examples 6.1 and 6.3, respectively. It can be concluded from these tables that, for both examples and all stopping criteria considered, the accuracy error $e_{\mathrm{L}^2(\Gamma_1)}(u_k)$ increases as $p_u$ and $p_q$ increase, hence the wGDM is stable with respect to decreasing the level of noise added to the Cauchy data. Furthermore, the number of iterations performed according to Morozov's discrepancy principle with either (6.5a) or (6.5b) and Hansen's L-curve method decreases with respect to increasing the amount of perturbation in the Cauchy. It should also be noted that, for Example 6.1, the best results in terms of accuracy have been obtained for the the L-curve method, followed by the discrepancy principle with (6.5a) and the same criterion with (6.5b), whereas the L-curve method provides more inaccurate reconstructions for the unknown data on $\Gamma_1$ than the discrepancy principle in case of Example 6.3.

### 6.3. Robustness of the wGDM

Next, we study the robustness of the wGDM with respect to the choice of the constant parameter $\gamma \equiv \gamma_k > 0$, $k \geq 0$. Table 3 presents the values of the accuracy error $e_{\mathrm{L}^2(\Gamma_1)}(u_k)$, the convergence error $E_{\Gamma_0}(u_k)$ and the number of iterations performed $k_{\mathrm{DP}}$, retrieved by the wGDM, the discrepancy principle with (6.5b), $n_{\mathrm{FEM}} = 756$, $p_u = p_q \in \{3\%, 5\%, 10\%\}$ and $\gamma \in \{10^{-4}, 10^{-5}, 10^{-6}\}$, for Example 6.2. It can be seen that, for all values of $\gamma$, the accuracy and convergence errors retrieved *via* the wGDM, in conjunction with Morozov's discrepancy principle, have precisely the same values for each amount of noise added to the Cauchy data, hence showing the robustness of the wGDM with respect to $\gamma$. Moreover, parameter $\gamma$ also has a relaxation effect on the wGDM since the iteration number required to retrieve the numerical solution according to each stopping rule employed decreases as $\gamma$ increases. At the same time, the wGDM is versatile since there is a broad range for the values of $\gamma$ that yield a convergent and stable solution.

Although not presented, it is reported that the proposed wGDM is also robust with respect to the initial guess for the unknown temperature on $\Gamma_1$, in the sense that for all examples investigated herein and each fixed FEM grid, the same accuracy in the wGDM-FEM approximations for both the temperature and the normal heat flux on $\Gamma_1$ is obtained for various constant initial guesses for $u|_{\Gamma_1}$.

TABLE 2. Values of the accuracy error $e_{\mathrm{L}^2(\Gamma_1)}(u_k)$, the corresponding convergence error $E_{\mathrm{SC}}$, given by $E_{\Gamma_0}(u_k)$, $E_{\mathrm{L}^2(\Gamma_0)}(u_k)$ or $E_{\mathrm{L}^2(\Gamma_0)}(q_k)$, and the number of iterations performed, $k_{\mathrm{SC}}$, retrieved by the wGDM, $\gamma = 10^{-3}$, $n_{\mathrm{FEM}} = 2856$, $p_u = p_q \in \{3\%, 5\%, 10\%\}$, the discrepancy principle (DP) with (6.5a) or (6.5b), and the L-curve method (LC), for Example 6.3.

| Stopping criterion | $p_u = p_q$ | $e_{\mathrm{L}^2(\Gamma_1)}(u_k)$ | $E_{\mathrm{SC}}$ | $k_{\mathrm{SC}}$ |
|---|---|---|---|---|
| DP & $E_{\Gamma_0}(u_k)$ | 3% | 4.22 (−1) | 3.44 (−1) | 1014 |
| | 5% | 4.35 (−1) | 5.05 (−1) | 633 |
| | 10% | 4.47 (−1) | 9.27 (−1) | 581 |
| DP & $E_{\mathrm{L}^2(\Gamma_0)}(u_k)$ | 3% | 4.22 (−1) | 8.75 (−2) | 1414 |
| | 5% | 4.22 (−1) | 1.07 (−1) | 1148 |
| | 10% | 4.35 (−1) | 1.69 (−1) | 800 |
| LC & $E_{\mathrm{L}^2(\Gamma_0)}(q_k)$ | 3% | 4.26 (−1) | 2.34 (−1) | 800 |
| | 5% | 4.31 (−1) | 2.99 (−1) | 700 |
| | 10% | 4.35 (−1) | 4.98 (−1) | 800 |

## 7. Conclusions

In this study, the inverse Cauchy problem associated with the Laplace-Beltrami equation has been investigated in a particular case, namely for a non-smooth/discontinuous anisotropic conductivity tensor. More precisely, the missing discontinuous/non-smooth thermal boundary conditions, *e.g.*, step functions like or $\mathrm{L}^2$–integrable boundary temperatures, on a portion of the boundary occupied by an anisotropic solid and the temperature distribution in the domain have been reconstructed from the knowledge of either exact or perturbed Cauchy data on the remaining boundary. To tackle this inverse problem in a rigorous manner, the notion of very weak solutions to a couple of direct problems of interest with $\mathrm{L}^2$–temperature data on the under-prescribed boundary was introduced, in the context of non-smooth/discontinuous anisotropic conductivity coefficients, following the approach of Marin [34]. Hence the original Cauchy problem was reformulated in terms of a control one which reduced to minimising an appropriate cost functional with respect to the $\mathrm{L}^2$–boundary temperature control. The latter minimisation problem was approached by an appropriate variational method which also enabled the computation of the gradient of the cost functional in a less regular framework and yielded a corresponding gradient-type method, namely the so-called wGDM, which is a weaker (*i.e.* relaxed) form of the GDM recently introduced by Bucataru *et al.* [11]. The proposed iterative algorithm is parameter-dependent and consists of two direct problems and their corresponding adjoint ones at each step. Using a non-standard analysis, it was proved that the wGDM generates a sequence of approximations of the solution which is convergent to the projection of the initial approximation on the set of admissible solutions, provided that the latter is non-empty. In spite of the parameter-dependent character of the proposed algorithm, an explicit admissible range for this parameter was also provided and this can be computed, at each iteration, with a reasonable computational cost.

The wGDM has been implemented numerically for homogeneous anisotropic solids in two dimensions using the FEM, whilst the convergence of the resulting FEM solution to the continuous one has also been proved. Both exact and noisy data have been considered on the over-prescribed and accessible boundary and two regularizing/stabilising stopping rules have also been provided for contaminated Cauchy data. The numerical results presented in Section 6 confirm that the combined FEM-wGDM developed, analysed and implemented in this study produces accurate, convergent and stable numerical reconstructions for both the missing discontinuous/non-smooth boundary conditions and the temperature distribution in the domain, in case of the Cauchy problem for the anisotropic Laplace equation with non-smooth/discontinuous conductivity coefficients, and is robust with respect to the initial guess for the Dirichlet data on the under-prescribed boundary. Future extensions of the

TABLE 3. Values of the accuracy error $e_{\mathrm{L}^2(\Gamma_1)}(u_k)$, the corresponding convergence error $E_{\mathrm{L}^2(\Gamma_0)}(u_k)$, and the number of iterations performed $k_{\mathrm{DP}}$, retrieved by the wGDM, $\gamma \in \{10^{-4}, 10^{-5}, 10^{-6}\}$, $n_{\mathrm{FEM}} = 756$, $p_u = p_q \in \{3\%, 5\%, 10\%\}$ and the discrepancy principle with (6.5b), for Example 6.2.

| $\gamma$ | $p_u = p_q$ | $e_{\mathrm{L}^2(\Gamma_1)}(u_k)$ | $E_{\Gamma_0}(u_k)$ | $k_{\mathrm{DP}}$ |
|---|---|---|---|---|
| $10^{-4}$ | 3% | 7.18 (−2) | 1.80 (−1) | 929 |
| | 5% | 8.16 (−2) | 3.00 (−1) | 614 |
| | 10% | 1.08 (−1) | 6.01 (−1) | 433 |
| $10^{-5}$ | 3% | 7.18 (−2) | 1.80 (−1) | 9288 |
| | 5% | 8.16 (−2) | 3.00 (−1) | 6138 |
| | 10% | 1.08 (−1) | 6.01 (−1) | 4322 |
| $10^{-6}$ | 3% | 7.18 (−2) | 1.80 (−1) | 92887 |
| | 5% | 8.16 (−2) | 3.00 (−1) | 61382 |
| | 10% | 1.08 (−1) | 6.01 (−1) | 43230 |

wGDM are currently under investigation and they refer to inverse Cauchy problems for the time-dependent anisotropic heat conduction and linear (an)isotropic (thermo)elasticity.

*Acknowledgements.* The work of Mihai Bucataru and Liviu Marin was supported by a grant of the Romanian Ministry of Research and Innovation, CNCS–UEFISCDI, project number PN–III–P1–1.1–TE–2019–0348, within PNCDI III, whilst the work of Iulian Cîmpean was supported by a grant of the Romanian Ministry of Research and Innovation, CNCS–UEFISCDI, project number PN–III–P1–1.1–PD–2019–0780, within PNCDI III.

## REFERENCES

[1] R. Aboulaïch, A. Ben Abda and M. Khallel, Missing boundary data reconstruction via an approximate optimal control. *Inverse Probl. Imaging* **2** (2008) 411–426.
[2] S. Agmon, Lectures on Elliptic Boundary Value Problems. Van Nostrand, Princeton (1965).
[3] S. Andrieux, A. Ben Abda and T.N. Baranger, Data completion via an energy error functional. *CR Mécanique* **333** (2005) 171–177.
[4] S. Andrieux, T.N. Baranger and A. Ben Abda, Solving Cauchy problems by minimizing an energy-like functional. *Inverse Probl.* **22** (2006) 115–133.
[5] M. Azaïez, F. Ben Belgacem, D.T. Du and F. Jelassi, A finite element model for the data completion problem: analysis and assessment. *Inverse Probl. Sci. Eng.* **19** (2011) 1063–1086.
[6] G. Baravdish, I. Borachok, R. Chapko, B.T. Johansson and M. Slodička, An iterative method for the Cauchy problem for second-order elliptic equations. *Int. J. Mech. Sci.* **142–143** (2018) 216–223.
[7] F. Ben Belgacem, D.T. Du and F. Jelassi, Local convergence of the Lavrentiev method for the Cauchy problem via a Carleman inequality. *J. Scientific Comput.* **53** (2012) 320–341.
[8] F. Ben Belgacem, V. Girault and F. Jelassi, Analysis of Lavrentiev-finite element methods for data completion problems. *Numer. Math.* **139** (2018) 1–25.
[9] F. Ben Belgacem, V. Girault and F. Jelassi, Full discretization of Cauchy's problem by Lavrentiev-finite element method. *SIAM J. Numer. Anal.* **60** (2022) 558–584.
[10] M. Berggren, Approximations of very weak solutions to boundary-value problems. *SIAM J. Numer. Anal.* **42** (2004) 860–877.
[11] M. Bucataru, I. Cîmpean and L. Marin, A gradient-based regularization algorithm for the Cauchy problem in steady-state anisotropic heat conduction. *Comput. Math. with Appl.* **119** (2022) 220–240.
[12] F. Caubet and J. Dardé, A dual approach to Kohn-Vogelius regularization applied to data completion problem. *Inverse Probl.* **36** (2020) 065008.
[13] A. Chakib and A. Nachaoui, Convergence analysis for finite element approximation to an inverse Cauchy problem. *Inverse Probl.* **22** (2006) 1191–1206.
[14] J. Dardé, Iterated quasi-reversibility method applied to elliptic and parabolic data completion problems. *Inverse Probl. Imaging* **10** (2016) 379–407.

[15] M. Essaouini, A. Nachaoui and S. El Hajji, Reconstruction of boundary data for a class of nonlinear inverse problems. *J. Inverse Ill-Posed Probl.* **12** (2004) 369–385.
[16] M. Essaouini, A. Nachaoui and S. El Hajji, Numerical method for solving a class of nonlinear elliptic inverse problems. *J. Comput. Appl. Math.* **162** (2004) 165181.
[17] D. Gilbarg and N.S. Trudinger, Elliptic Partial Differential Equations of Second Order. Springer-Verlag, Berlin (1983).
[18] M. Gockenbach, Understanding and Implementing the Finite Element Method. SIAM, Philadelphia (2006).
[19] Y. Gu, W. Chen and Z.-J. Fu, Singular boundary method for inverse heat conduction problems in general anisotropic media. *Inverse Probl. Sci. Eng.* **22** 889–909 (2014).
[20] Y. Gu, W. Chen, C. Zhang and X. He, A meshless singular boundary method for three-dimensional inverse heat conduction problems in general anisotropic media. *Int. J. Heat Mass Trans.* **84** (2015) 91–102.
[21] A. Habbal and M. Khallel, Data completion problems solved as Nash games. *J. Phys. Conf. Ser.* **386** (2012) 012004.
[22] A. Habbal and M. Khallel, Neumann-Dirichlet Nash strategies for the solution of elliptic Cauhcy problems. *SIAM J. Control Optim.* **51** (2013) 4066–4083.
[23] J. Hadamard, Lectures on Cauchy Problem in Linear Partial Differential Equations. Yale University Press, New Haven (1923).
[24] M. Hanke and P.C. Hansen, Regularization methods for large-scale problems. *Surv. Math. Industry* **3** (1993) 253–315.
[25] P.C. Hansen, The L-curve and its use in the numerical treatment of inverse problems. *Comput. Inverse Probl. Electrocardiol.* **4** (2001) 119–142.
[26] D.N. Hào, B.T. Johansson, D. Lesnic and P.M. Hien, A variational method and approximations of a Cauchy problem for elliptic equations. *J. Algorithm Comput. Technol.* **4** (2010) 89–119.
[27] L. Hörmander, The Analysis of Partial Differential Operators I. Springer-Verlag, Berlin (2003).
[28] B. Jin, Y. Zheng and L. Marin, The method of fundamental solutions for inverse boundary value problems associated with the steady-state heat conduction in anisotropic media. *Int. J. Numer. Methods Eng.* **65** (2006) 1865–1891.
[29] T. Johansson, An iterative procedure for solving a Cauchy problem for second order elliptic equations. *Math. Nachr.* **272** (2004) 46–54.
[30] V.A. Kozlov, V.G. Mazya and A.V. Fomin, An iterative method for solving the Cauchy problem for elliptic equations. *Zhurnal Vychislitelnoi Matematiki i Matematicheskoi Fiziki* **31** (1991) 64–74. English translation: *U.S.S.R. Comput. Math. Math. Phys.* **31** (1991) 45–52.
[31] C. Ma, Z. Ma, L. Gao, Y. Liu, T. Wu, L. Wang, C. Wei and F. Wan, Preparation and characterization of coatings with anisotropic thermal conductivity. *Mater. Des.* **160** (2018) 1273–1280.
[32] L. Marin, An alternating iterative MFS algorithm for the Cauchy problem in two-dimensional anisotropic heat conduction. *CMC: Comput. Mater. Contin.* **12** (2009) 71–100.
[33] L. Marin, Stable boundary and internal data reconstruction in two-dimensional anisotropic heat conduction Cauchy problems using relaxation procedures for an iterative MFS algorithm. *CMC: Comput. Mater. Contin.* **17** (2010) 233–274.
[34] L. Marin, Landweber-Fridman algorithms for the Cauchy problem in steady-state anisotropic heat conduction. *Math. Mech. Solids* **25** (2020) 1340–1363.
[35] L. Marin, An iterative algorithm for the Cauchy problems associated with the steady-state anisotropic heat conduction, in *Current Trends in Applied Mathematics, Iaşi, Romania, 21–22 September, 2020.*
[36] J. Marschall, The trace of Sobolev-Slobodeckij spaces on Lipschitz domains. *Manuscripta Math.* **58** (1987) 47–65.
[37] N.S. Mera, L. Elliott, D.B. Ingham and D. Lesnic, The boundary element solution for the Cauchy steady heat conduction problem in an anisotropic medium. *Int. J. Numer. Methods Eng.* **49** (2000) 481–499.
[38] N.S. Mera, L. Elliott, D.B. Ingham and D. Lesnic, An iterative algorithm for singular Cauchy problems for the steady state anisotropic heat conduction equation. *Eng. Anal. Bound. Elem.* **26** (2002) 157–168.
[39] V.A. Morozov, On the solution of functional equations by the method of regularization. *Doklady Math.* **167** (1966) 510–512.
[40] M.N. Özişik, Heat Conduction. John Wiley & Sons, New York (1993).
[41] R. Rischette, T.N. Baranger and N. Debit, Numerical analysis of an energy-like minimization method to solve the Cauchy problem with noisy data. *J. Comput. Appl. Math.* **235** (2011) 3257–3269.
[42] R. Rischette, T.N. Baranger and S. Andrieux, Regularization of the noisy Cauchy problem solution approximated by an energy-like method. *Int. J. Numer. Methods Eng.* **95** (2013) 271–287.
[43] F. Riesz and B.S. Nagy, Functional Analysis. Dover Publications Inc. (Verlag), New York (1990).
[44] O. Steinbach, Numerical Approximation Methods for Elliptic Boundary Value Problems. Springer-Verlag, New York (2008).
[45] S. Trevisan, W. Wang and B. Laumert, Coatings utilization to modify the effective properties of high temperature packed bed thermal energy storage. *Appl. Therm. Eng.* **185** (2021) 116414.
[46] A.-P. Voinea-Marinescu, L. Marin and F. Delvare, BEM-fading regularization algorithm for Cauchy problems in 2D anisotropic heat conduction. *Numer. Algorithms* **88** (2021) 1667–1702.

[47] A.-P. Voinea-Marinescu and L. Marin, Fading regularization MFS algorithm for the Cauchy problem in anisotropic heat conduction. *Comput. Mech.* **68** (2021) 921–941.